Widespread pollution events of carbon monoxide observed over the western North Pacific during the East Asian Regional Experiment (EAREX) 2005 campaign

Yousuke Sawa,[1] Hiroshi Tanimoto,[2] Seiichiro Yonemura,[3] Hidekazu Matsueda,[1] Akira Wada,[1] Shoichi Taguchi,[4] Tadahiro Hayasaka,[5] Haruo Tsuruta,[6] Yasunori Tohjima,[2] Hitoshi Mukai,[7] Nobuyuki Kikuchi,[5,8] Syuichiro Katagiri,[5] and Kazuhiro Tsuboi[9]

[1] Temporal variations of carbon monoxide (CO) were observed simultaneously at seven surface stations located in east Asia/western North Pacific from 24°N to 43°N during the East Asian Regional Experiment (EAREX) 2005 campaign in March 2005. Three major pollution events with enhanced CO levels were recorded around the same time at four stations over the East China Sea and at two northern stations of Japan. These pollution events were also observed 3–4 d later at Minamitorishima, located far from the Asian continent. A synoptic weather analysis showed that all of the major CO enhancements were brought about by the passages of cold fronts associated with the eastward migrating cyclonic development. The CO distribution simulated by a three-dimensional transport model showed that the polluted air masses exported from the continent were trapped behind the cold fronts and then merged into elongated belts of enriched CO before spreading over the western North Pacific. Transport of regionally tagged CO tracer simulated by the model indicated that the Chinese and Korean emissions were the major contributors to the pollution over the East China Sea, while the Japanese emissions had impacts at relatively higher latitude regions during the campaign. The simulation results also showed that the CO enhancements detected at Minamitorishima were caused by a long-range transport of pollution emissions from various regions in east Asia. The CO-enriched plumes from Southeast Asia and south Asia emissions were found above the boundary layer in the frontal zone but not at the surface.

Citation: Sawa, Y., et al. (2007), Widespread pollution events of carbon monoxide observed over the western North Pacific during the East Asian Regional Experiment (EAREX) 2005 campaign, *J. Geophys. Res.*, *112*, D22S26, doi:10.1029/2006JD008055.

1. Introduction

[2] East Asia is a major source region for anthropogenic trace gases and aerosols associated with urban/industrial emissions and biomass burnings [*Streets et al.*, 2003]. Anthropogenic emissions from human activities in east Asia increased rapidly from 1970s to 1980s [*Kato and Akimoto*, 1992], with a reduction in the growth rate during the late 1990s [*Streets et al.*, 2001a, 2001b]. In the future, the east Asian regions will continue to share a large portion of the global anthropogenic emissions of carbon monoxide (CO).

[3] *Tanimoto et al.* [2005] pointed out that the regional air quality over the western North Pacific is largely influenced by the transport of anthropogenic emissions from Asia. CO has been used as a key tracer in identifying the influence of Asian pollution outflow over the western North Pacific [e.g., *Jaffe et al.*, 1997]. In addition to the observations of episodic CO events at several remote island stations of Okinawa [*Akimoto et al.*, 1996], Oki [*Jaffe et al.*, 1996; *Kajii et al.*, 1997; *Pochanart et al.*, 1999] and Rishiri [*Tanimoto et al.*, 2000, 2002] in Japan, a long-range transport of Asian pollution was identified in the CO data obtained at remote stations operated by National Oceanic and Atmospheric Administration/Global Monitoring Divi-

[1]Geochemical Research Division, Meteorological Research Institute, Tsukuba, Japan.
[2]Atmospheric Environmental Division, National Institute for Environmental Studies, Tsukuba, Japan.
[3]National Institute for Agro-Environmental Sciences, Tsukuba, Japan.
[4]Research Institute for Environmental Management Technology, National Institute of Advanced Industrial Science and Technology, Tsukuba, Japan.
[5]Research Institute for Humanity and Nature, Kyoto, Japan.

[6]Center for Climate System Research, University of Tokyo, Kashiwa, Japan.
[7]Center for Global Environmental Research, Institute for Environmental Management Technology, National Institute for Environmental Studies, Tsukuba, Japan.
[8]Now at Earth Observation Research Center, Japan Aerospace Exploration Agency, Tsukuba, Japan.
[9]Atmospheric Environmental Division, Japan Meteorological Agency, Tokyo, Japan.

sion (NOAA/GMD, former NOAA/CMDL) [*Jaffe et al.*, 1997, 1998]. A number of intensive field missions using research aircrafts, such as PEM-West A and B [*Hoell et al.*, 1996, 1997], ACE-Asia [*Huebert et al.*, 2003], TRACE-P [*Jacob et al.*, 2003], BIBLE [*Kondo et al.*, 2002] and PEACE [*Kondo et al.*, 2004] have also been carried out, demonstrating the pervasive influence from the anthropogenic Asian emissions have on the composition of the Pacific troposphere, affecting both the aerosol loading and the ozone photochemistry [e.g., *Crawford et al.*, 1997; *Talbot et al.*, 1997; *Browell et al.*, 2003].

[4] Several previous studies have examined some of the main transport processes. A combination of fast convective transport [*Folkins et al.*, 1997; *Bey et al.*, 2001] or orographic lifting [*Liu et al.*, 2003] with strong westerly flow are known to contribute to the long-range transport of Asian pollution over the western Pacific. Cold fronts associated with the eastward traveling cyclonic systems have also been shown to be one of the major transport mechanisms [*Carmichael et al.*, 1998; *Yienger et al.*, 2000; *Bey et al.*, 2001; *Liu et al.*, 2003]. Although many of the recent studies associated with the cold front mechanism focused on the role of warm conveyor belts (WCB) for exporting pollution from the boundary layer into the free troposphere [*Stohl*, 2001; *Liu et al.*, 2003; *Miyazaki et al.*, 2003; *Mari et al.*, 2004], others showed that cold fronts play an important role in boundary layer outflow [*Bey et al.*, 2001; *Liang et al.*, 2004]. Even though the aircraft measurements, combined with analyses using chemical transport models (CTM), have revealed vertical CO distributions across fronts [e.g., *Cooper et al.*, 2004; *Takigawa et al.*, 2005], studies focusing on the boundary layer outflow based on the observational results are still limited.

[5] Continuous measurements of atmospheric chemical species at ground-based stations remain an important strategy in understanding the transport mechanism of the boundary layer outflows associated with cold front activities. *Liu et al.* [1997] observed a sharp CO increase at the surface after the passage of a front in Taiwan during the PEM-West B campaign. Frontal transport of CO was also reported at other stations in the western North Pacific Rim, such as Hong Kong [*Chung et al.*, 1999] and Yonagunijima [*Yamada*, 1999]. On the basis of their CTM interpretation of the continuous CO data at Cheeka Peak observatory on the west coast of the United States, *Liang et al.* [2004] concluded that the majority of enhanced CO events observed in the eastern North Pacific region are mainly due to the transoceanic boundary layer transport. However, a study of storm tracks over the northern hemisphere showed that a very few synoptic systems can be tracked across the width of the Pacific basin [*Hoskins and Hodges*, 2002]. Observational evidence about how far the boundary layer transport can reach has been rarely reported so far. Because long-range transport mechanisms are very complex, we need to obtain as much as possible observational data of chemical species such as CO to evaluate the spatial extent of pollution over time, as well as to understand the detailed mechanisms of the continental outflow of pollutants from Asia. This can be achieved by making simultaneous high-resolution ground-based CO measurements at different stations located in the western Pacific.

[6] The East Asian Regional Experiment (EAREX) 2005 was organized under the UNEP/ABC-Asia project [*Ramanathan and Crutzen*, 2003] (see also http://www-abc-asia.ucsd.edu) to set up a well-coordinated network of stations to monitor pollutants transported off Asia. The major objectives of the ABC-Asia included understanding the effects of air pollution and mineral dust in the Asian region to the Earth's climate and environment [*Nakajima and Yoon*, 2005]. The international cooperative observations for the EAREX 2005 campaign were made at Gosan station in Korea during March 2005. We participated in this campaign as a Japanese collaborative group that included scientists from the Meteorological Research Institute (MRI), the National Institute for Environmental Studies (NIES), and the National Institute for Agro-Environmental Sciences (NIAES). These collaborative measurements have provided us with an opportunity to obtain a consistent data set of CO and ozone (O_3) from several other observational stations that can be used intercomparatively with the data from the Gosan station [*Tanimoto et al.*, 2007].

[7] In this study, we have focused our analysis on several episodic enhanced CO events observed at Gosan and other ground-based monitoring stations operated by several different programs in Japan during the EAREX 2005 campaign. First, the spatial extent of pollution plumes associated with the episodic events are shown and discussed. Secondly, continental outflows of enhanced CO for the pollution events are examined within the context of the associated meteorological conditions. Thirdly, dispersion of pollution plumes associated with the CO events and the underlying transport mechanisms are examined using a three-dimensional (3-D) transport model. The importance of transport processes associated with evolving cold fronts in exporting pollution out of the Asian continent is also highlighted.

2. Experimental Section
2.1. Observation Sites

[8] The EAREX 2005 campaign was conducted from the end of February to early April 2005 as a part of international intercomparison experiments on the basis of CO and O_3 measurements; it involved collaboration of four Asian research groups from Japan, Korea, Hong Kong and Taiwan. During the campaign, we observed CO and O_3 concentrations at Gosan station (33°17′N, 126°10′E) located at Jeju Island in Korea. The Gosan station is one of the UNEP/ABC supersites operated by the Meteorological Research Institute (METRI) in the Korea Meteorological Administration (KMA). Although preliminary results from this intercomparison experiment in the EAREX 2005 will be published elsewhere in detail, the ambient air measurements from the different research groups at Gosan agree with each other relatively well [*Tanimoto et al.*, 2007].

[9] In order to investigate the spatiotemporal variations of CO, the CO data obtained at the six Japanese stations are compared to those at Gosan for the same period of time. Figure 1 shows the geographical distribution of the stations used in the present study. The geographical distribution of these stations is suitable for examining the spread of pollution over the western North Pacific Rim between 43°N to 24°N from the Asian continent. All these 7 surface
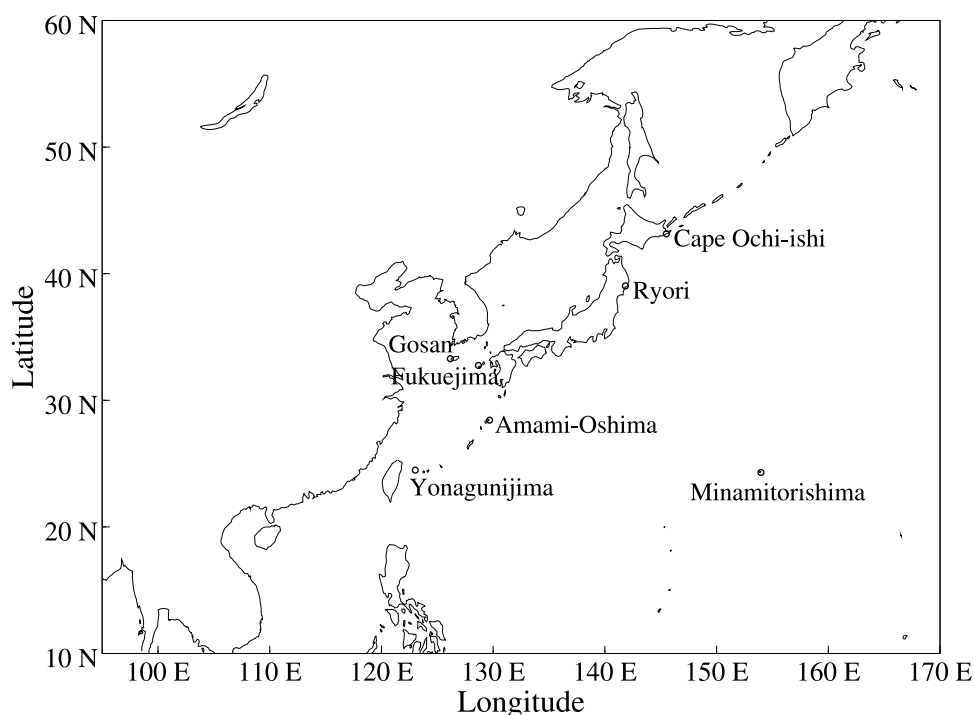
Figure 1. Location of CO monitoring stations used in this study.

stations are generally situated in rural regions where the influences of local CO emissions are negligible.

[10] The Fukuejima station (32°45′N, 128°41′E) located west of Japan is closest to the Gosan station, while the Amami-Oshima station (28°26′N, 129°41′E) is located to the south of Gosan station. At these two island stations, CO and O_3 measurements were collaboratively performed by NIAES, the Research Institute for Humanity and Nature (RIHN), and the Center for Climate System Research (CCSR) under the aerosol research programs of SKYNET and NIES LidarNet.

[11] The Japan Meteorological Agency (JMA) has been monitoring CO, O_3 and other trace gases at Yonagunijima (24°28′N, 123°01′E), Minamitorishima (24°17′N, 153°39′E), and Ryori (39°02′N, 141°49′E) for the Global Atmosphere Watch program of the World Meteorological Organization (WMO/GAW). The observational data at these JMA stations are available on the Web site of the World Data Center for Greenhouse Gases (WDCGG) operated by JMA (http://gaw.kishou.go.jp/wdcgg.html). Note that Minamitorishima is located the farthest and to the southeast of Gosan (and the Asian continent). Trace gas measurements at Cape Ochi-ishi station (43°09′N, 145°30′E), which is located at the northernmost position in the network, are conducted by NIES for the CGER Global Environmental Monitoring Program [e.g., *Tohjima et al.*, 2002].

2.2. CO Measurement Systems

[12] CO concentrations at Gosan were measured using a nondispersive infrared analyzer (NDIR from Horiba APMA-360 model) with a sample air flow of about 1 L/min. The NDIR analyzer was regularly calibrated using a CO-free air and CO standard gas with a concentration of about 1 ppm. The CO-free air was produced by passing ambient air through a catalytic oxidation column packed with Sofnocat (514,

Molecular Products Ltd., UK) to completely remove CO in the sample air. The CO content in the standard gas filled in a 10-L high-pressure cylinder was determined before and after the observations using 5 gravimetric standard gases prepared as a MRI primary scale [*Matsueda et al.*, 1998]. The NDIR system used at Gosan was further tested at our laboratory in reference to CO measurements by a high-precision method using a gas chromatograph (GC) equipped with a HgO detector (TRA-1 model, Round-Science Co. Ltd., Japan). The comparisons showed that an overall uncertainty of the NDIR system was estimated to be less than 20 ppb.

[13] Measurements of CO at Fukuejima and Amami-Oshima stations were made by the gas filter correlation method (GFC) using commercially available CO analyzers (TEI model 48C, Thermo Electron Inc., USA) combined with zero-air generators of CO-free air (TEI model 111, Thermo Electron Inc., USA). The GFC analyzers at both stations were regularly calibrated using one CO standard gas of about 1 ppm. The amount of CO in the standard gas was assigned by the same MRI primary standard scale used at Gosan station in order to produce a consistent data set. From the comparison with the GC/HgO method at NIAES, an overall uncertainty of the GFC method was estimated to be about 10 ppb. On the other hand, JMA used NDIR analyzers (GA-360S model, Horiba Co. Ltd., Japan) for CO measurements at their three WMO/GAW stations. The JMA CO system was reported elsewhere in detail [*Japan Meteorological Agency (JMA)*, 1994; *Watanabe et al.*, 2000]. A previous intercomparison of ambient CO measurements between JMA and MRI showed a systematic difference of about 10 ppb mainly because of the standard gas scale. Since this difference was relatively small compared to the large analytical error from the NDIR method, CO values from the JMA system were not corrected. At
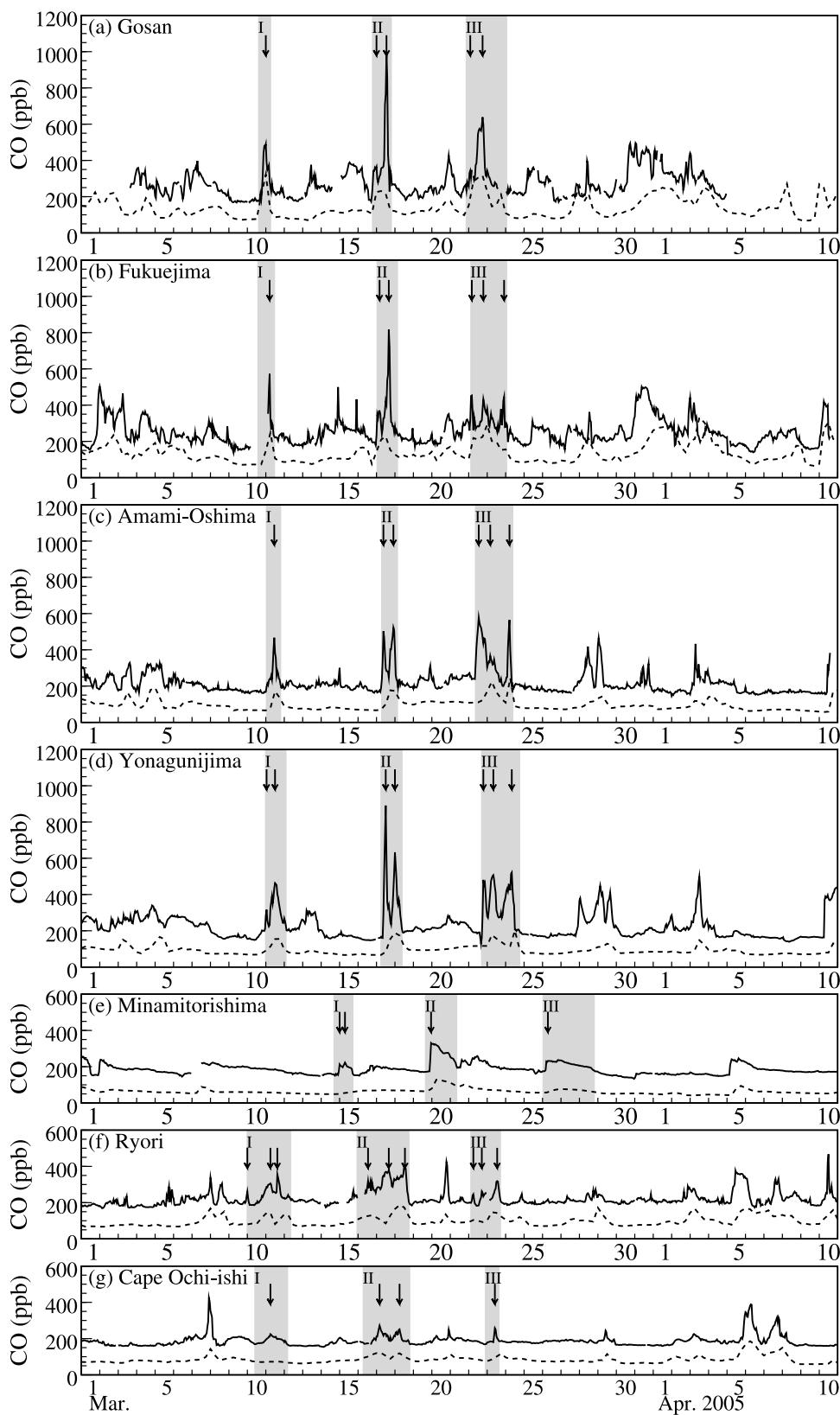
Figure 2. Time series of hourly CO mixing ratios observed at seven stations from March to April in 2005 (solid lines): (a) Gosan, (b) Fukuejima, (c) Amami-Oshima, (d) Yonagunijima, (e) Minamitorishima, (f) Ryori, and (g) Cape Ochi-ishi. Shaded regions indicated three significant enhanced CO events (events I, II, and III). The arrows show the observed CO peaks in the events. CO mixing ratios simulated by the model every 6 h are shown with dashed lines. For Fukuejima, one grid east from the original point was shown. Time units are UTC.

Table 1. Enhanced CO Events Observed at Stations in the East China Sea During the EAREX 2005

Station	Period	First Peak			Second Peak			Third Peak		
		Date	CO, ppb	Delay, h	Date	CO, ppb	Delay, h	Date	CO, ppb	Delay, h
Event I										
Gosan	10 Mar 1400 UT to 11 Mar 0700 UT				11 Mar 0000 UT	490				
Fukuejima	10 Mar 1300 UT to 11 Mar 1200 UT				11 Mar 0500 UT	565	5			
Amami-Oshima	11 Mar 0000 UT to 11 Mar 2000 UT				11 Mar 1100 UT	466	11			
Yonagunijima	10 Mar 2300 UT to 12 Mar 0300 UT	11 Mar 0100 UT	316		11 Mar 1200 UT	463	12			
Event II										
Gosan	16 Mar 1800 UT to 17 Mar 2000 UT	17 Mar 0000 UT	365		17 Mar 1300 UT	997				
Fukuejima	17 Mar 0000 UT to 18 Mar 0400 UT	17 Mar 0400 UT	368	4	17 Mar 1600 UT	824	3			
Amami-Oshima	17 Mar 0600 UT to 18 Mar 0400 UT	17 Mar 0900 UT	502	9	17 Mar 2200 UT	522	9			
Yonagunijima	17 Mar 0500 UT to 18 Mar 1000 UT	17 Mar 1200 UT	891	12	18 Mar 0000 UT	633	11			
Event III										
Gosan	21 Mar 2000 UT to 24 Mar 0200 UT	22 Mar 0200 UT	343		22 Mar 1800 UT	639				
Fukuejima	22 Mar 0200 UT to 24 Mar 0200 UT	22 Mar 0400 UT	452	2	22 Mar 1900 UT	435	1	23 Mar 2200 UT	457	(0)
Amami-Oshima	22 Mar 0800 UT to 24 Mar 1000 UT	22 Mar 1300 UT	578	11	23 Mar 0400 UT	366	10	24 Mar 0500 UT	566	(7)
Yonagunijima	22 Mar 1600 UT to 24 Mar 1900 UT	22 Mar 1900 UT	481	17	23 Mar 0800 UT	507	14	24 Mar 0800 UT	521	(10)

Cape Ochi-ishi station, the CO data were obtained by the GC/HgO (RGD2, Trace Analytical Co. Ltd., USA) method on the basis of the NIES scale derived from gravimetric CO standard gases. It was concluded that the hourly CO data from all of the stations used in this study were comparable within an overall uncertainty of about 20–30 ppb.

2.3. Three-Dimensional CO Tracer Simulation

[14] To investigate the mechanism of the spatial and temporal variations of CO observed in this study, we use a 3-D chemical transport model (STAG-NCAR/NCEP developed from model NIRE-CTM 96) by the National Institute of Advance Industrial Science and Technology (AIST, former NIRE) [*Taguchi*, 1996; *Taguchi et al.*, 2002a]. Since details of the model have been reported elsewhere [*Sawa*, 2005], only a brief description of the CO model calculation procedure is given here. This model, which consists of 28 sigma (σ) vertical levels with T63 (equivalent to 1.8×1.8 degrees resolution) horizontal grid, is driven every 6 h using the meteorological reanalysis data provided by the NOAA-CIRES Climate Diagnostics Center at their Web site at http://www.cdc.noaa.gov/. The boundary layer stability at each time step of the model is estimated from the bulk Richardson number [*Troen and Mahrt*, 1986] and is used to calculate the boundary layer height and the uniform distribution of CO concentration in the layer. The basic performance of the model has been evaluated by using radon-222 concentrations [*Taguchi et al.*, 2002b]. CO is emitted from all anthropogenic sources compiled in the Emission Database for Global Atmospheric Research

(EDGAR) 3.2 Fast Track 2000 data set [*Olivier et al.*, 1999, 2005; *Olivier and Berdowski*, 2001]. Biomass burning emissions are changed in the model from the monthly varying climatological inventory, while other CO emissions are based on the yearly values in the database. Other major CO sources such as photochemical production via the oxidation of methane and nonmethane hydrocarbons (NMHCs) are not included in this study. Photochemical destruction of CO with OH is included in the model as the only CO sink, with an assigned climatological seasonal fields of OH radicals obtained from *Spivakovsky et al.* [2000].

3. Results and Discussion

3.1. CO Variations

[15] Figure 2a shows temporal variations of hourly mean CO observed at Gosan station for about one month from 3 March to 5 April in 2005. In the early spring, the observed CO concentration varied mostly in the range of 170 to 400 ppb, with a few large episodic events showing peaks 500 to 1000 ppb. Background levels of CO during this season were around 200 ppb, similar to the CO levels in clean air observed at similar latitudes at the NOAA/GMD sampling network [e.g., *Novelli et al.*, 1992, 1998, 2003]. However, a mean CO value for the observational period was calculated to be about 290 ppb because of the frequent events of enhanced CO concentration. In particular, four major episodic events with large CO increases of more than 400 ppb were observed during 10–11, 16–17, and 22–24 March and 30 March to 2 April. The CO enhancements

(a) Event-I   (b) Event-II   (c) Event-III
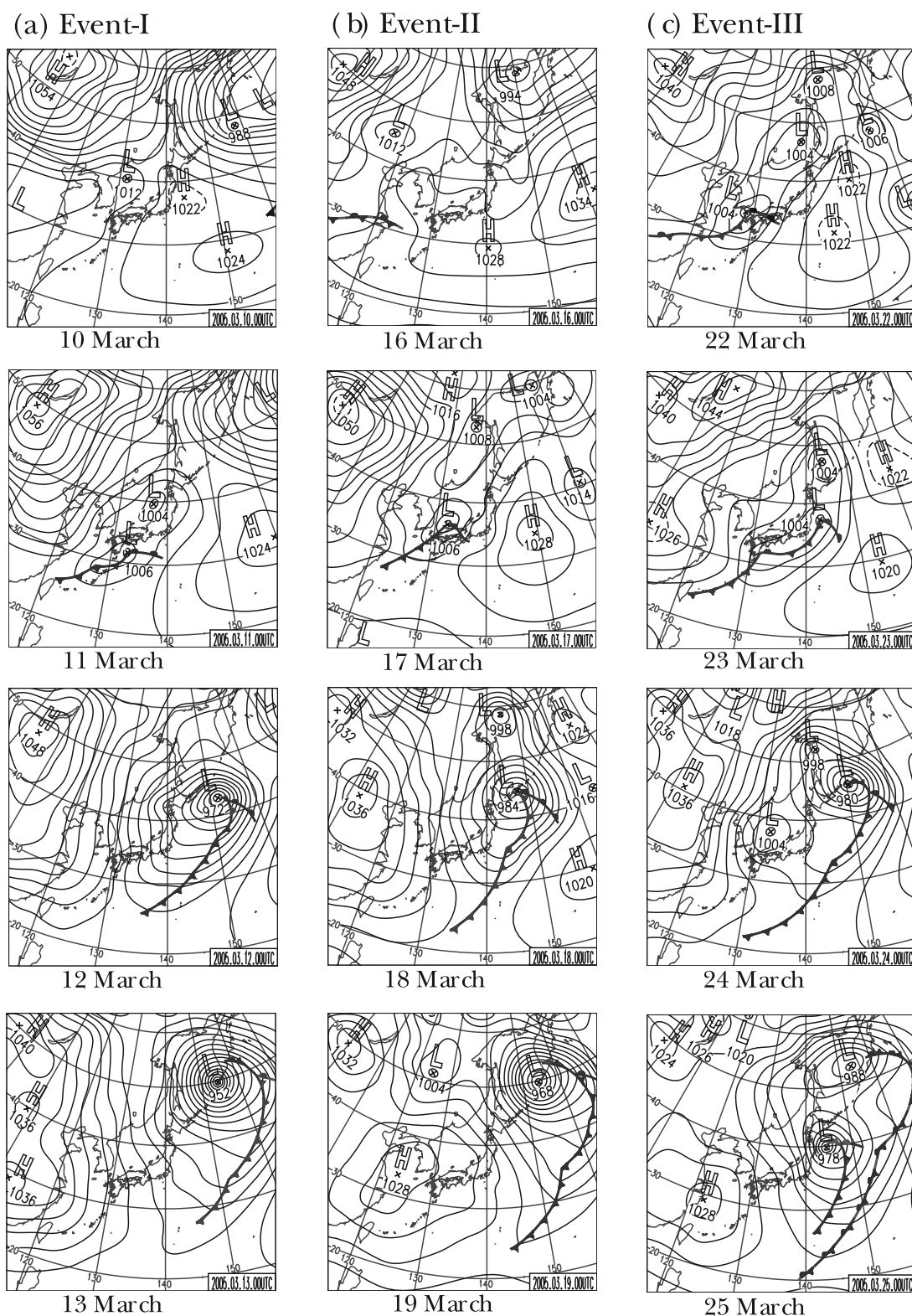
Figure 3. Time series of the surface weather charts of the east Asia and the western North Pacific regions on (a) 10–13 March, (b) 16–19 March, and (c) 22–25 March 2005. Time units are UTC.

occurred with a time interval of several days and often lasted for 1–2 d.

[16] The CO levels at Fukuejima also show a similar variation as observed at Gosan because of its proximity to Gosan. The enhanced CO levels for the four episodic events mentioned above can also be seen at Fukuejima (Figure 2b), indicating influence of transport rather than local anthropogenic emissions.
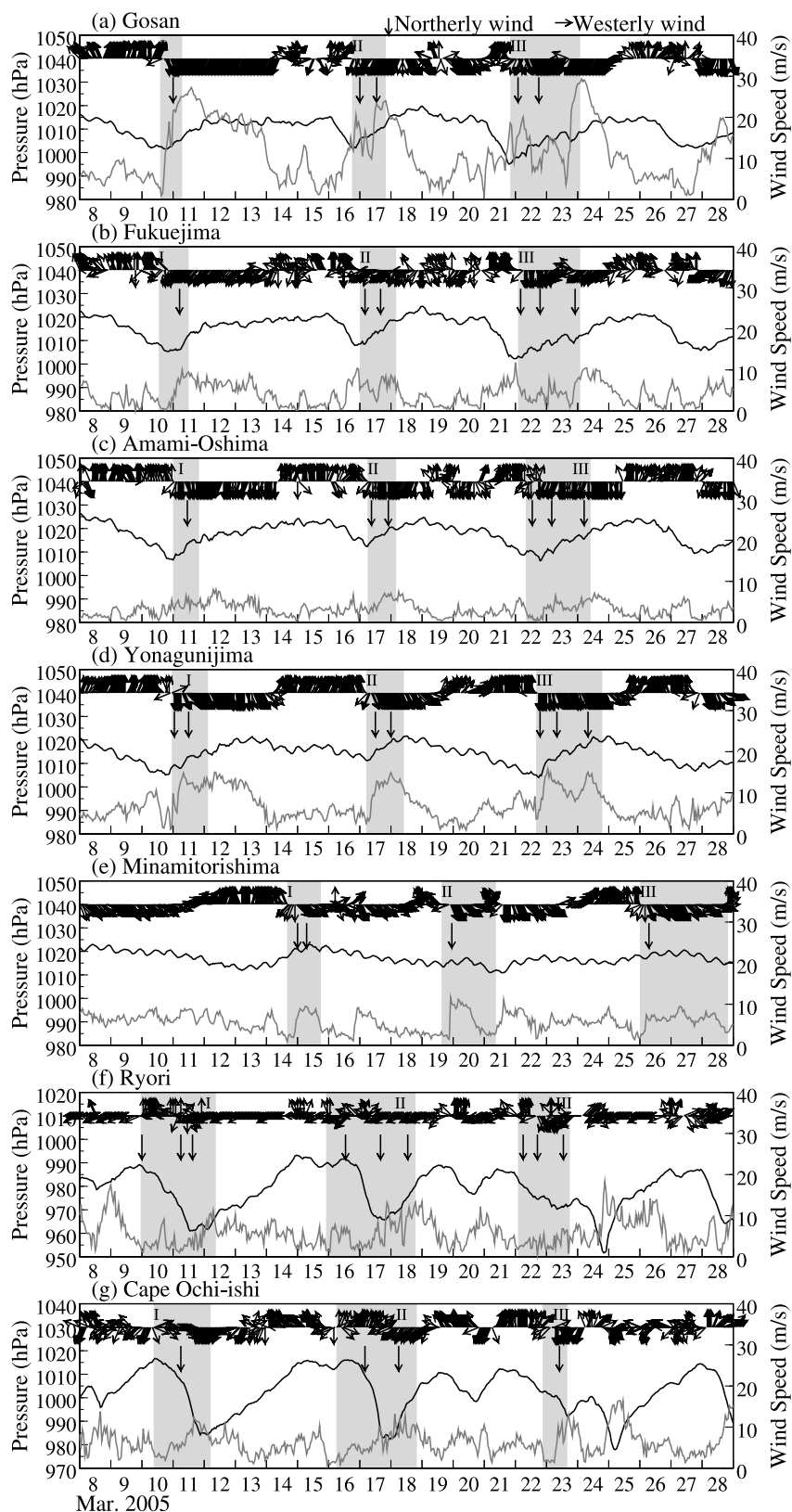
Figure 4. Time series of in situ surface pressure (black) and wind speeds (gray) in March 2005 at (a) Gosan, (b) Fukuejima, (c) Amami-Oshima, (d) Yonagunijima, (e) Minamitorishima, (f) Ryori, and (g) Cape Ochi-ishi. Wind directions are plotted by the arrows. Shaded regions and arrows indicate three significant enhanced CO events and the observed CO peaks. Semidiurnal variations of pressure at the southern stations were caused by atmospheric tides in the low latitudes [e.g., *Haurwitz and Cowley*, 1973]. Time units are UTC.

[17] Variations in CO observed at other stations (Figures 2c–2g) show the regional extent of the events seen at Gosan. The three major episodic CO events of 11, 17–18, and 22–24 March observed at Gosan were also detected at Amami-Oshima (Figure 2c). Yonagunijima is located in the subtropical region far form the Gosan station, but it is of interest that the CO variation at this station (Figure 2d) shows a similar pattern as the one observed at Gosan. Insignificant diurnal variations of CO were found at these stations in the East China Sea. On the other hand, similarities in the observed CO time series, including episodic events, among these geographically separated stations strongly indicate atmospheric transport of polluted air masses eastward from the Asian continent.

[18] In the present study, we focus on three major CO-enhanced events and they are identified as event I (10–12 March), II (16–18 March), and III (22–24 March). These events, which are shown in shaded regions in Figure 2, were chosen because these events were observed at all stations and consequently provide a database for model analysis of mechanism of long-range transport of pollution off the Asian continent. These three events also reflect the salient features of the relationship between the basic air pollution transport and the location of the pollution emission that cause other CO events shown in Figure 2. Since two or three increased CO peaks are identified during each event, their timings are summarized in Table 1. These increased CO peaks are defined as IC peaks in the present study. The differences in the timing of IC peak occurrences were observed among stations. For example, in event I, the major CO peak occurred at Amami-Oshima and Yonagunijima about half a day after it was observed at Gosan, indicating advective transport from north to south over the East China Sea.

[19] A similar delay in IC peaks was also observed for event II which is characterized by two major peaks of similar magnitude at Amami-Oshima and Yonagunijima. The first peak was comparatively much smaller at Gosan and Fukuejima. For event III, the CO enhancement at Fukuejima, Amami-Oshima, and Yonagunijima is characterized by three separate but closely packed peaks. The sequence of IC peak occurrence and the meteorological data at these stations are consistent with north to south transport of pollutants, as discussed in sections 3.2 and 3.3. The third peak was observed at Fukuejima, but not at Gosan. Given the similarity in the CO variation between Gosan and Fukuejima and the close location of the latter to the former, it is our contention that Gosan would have detected the third peak had it not been for the trouble with the measuring instrument caused by a power failure at the time of the occurrence of the third peak.

[20] The CO variation at Minamitorishima is relatively small because of its distant location to the east of other station. However, events I, II and III were still detected at the station 3–4 d after being observed over the East China Sea, but with reduced CO values of about 250–300 ppb (Figure 2e). The details of the long-range transport of CO to Minamitorishima will be discussed later within the context of 3-D transport model simulations.

[21] Since Ryori and Cape Ochi-ishi are located to the north of Gosan, they are useful for examining outflows of pollutants toward the northern North Pacific regions. Events I and II were also detected at Ryori, but at a slightly earlier time than at Gosan; the overall nature of the CO variation observed at Ryori is different from those observed at the southern stations, and was likely caused by local anthropogenic emissions in Japan (Figure 2f). Cape Ochi-ishi in the northern part of Japan shows a relatively low variation in the CO concentration (Figure 2g), but there are several IC peaks which appear to be related to events I, II and III. Observations at these two northerly stations indicate advection to the northern North Pacific region of some of the episodic pollution events observed at Gosan. Results of transport model simulations, to be discussed later, will show in detail how this is possible.

3.2. Synoptic-Scale Weather Change

[22] We now describe the general synoptic meteorological conditions that existed during the three major pollution events identified in the previous section (Figure 2). Figure 3a shows the daily weather charts [JMA, 2005b] over the western North Pacific from 10 to 13 March associated with event I. The Pacific High was located to the southeast of Japan before event I at 0000 UTC on 10 March. The weather condition changed on 11 when the CO concentration began to increase. This change was caused mainly by the appearance of a cyclone with a cold front stretching southwestward over the East China Sea. The weather charts for 12 and 13 March indicate the deepening of the low with intensifying cold front as it moved northeastward.

[23] A similar synoptic weather evolution was associated with the occurrence of events II and III (Figures 3b and 3c). An interesting difference in event III from the previous events is the cyclogenesis of a second low system over the Sea of Japan on 24 March after the first low moved off northeastward. Each of the relevant lows shown in Figure 3 was associated with an identifiable cold front.

3.3. Meteorological Parameters

[24] Associated with the synoptic weather evolution described above were local changes in the meteorological parameters observed at each of the CO monitoring stations. The data for the Japanese stations were obtained from the closest JMA weather observatories [JMA, 2005a], while the meteorological parameters at Gosan were derived from the Automatic Weather Station data in KMA/METRI [Nam and Bang, 2005]. Figure 4 shows the time series of pressure, wind direction, and wind speed observed at Gosan, Fukuejima, Amami-Oshima, Yonagunijima, Minamitorishima, Ryori and Cape Ochi-ishi. For the four stations of Gosan, Fukuejima, Amami-Oshima, and Yonagunijima in the East China Sea, a decrease in pressure accompanied by a rapid change in the wind direction, and a subsequent increase in the wind speed were commonly observed when an IC event occurred (Figures 4a–4d). During each event, first IC peak corresponded to a pressure decrease and a rapid change in the wind direction from southerly to northerly, which is indicative of a cold frontal passage. These results suggest that the first CO peak was brought about by a sudden change in the air mass at the station from a clean maritime air to a continental polluted air immediately after the cold front had passed. After the passage of the cold front, the second
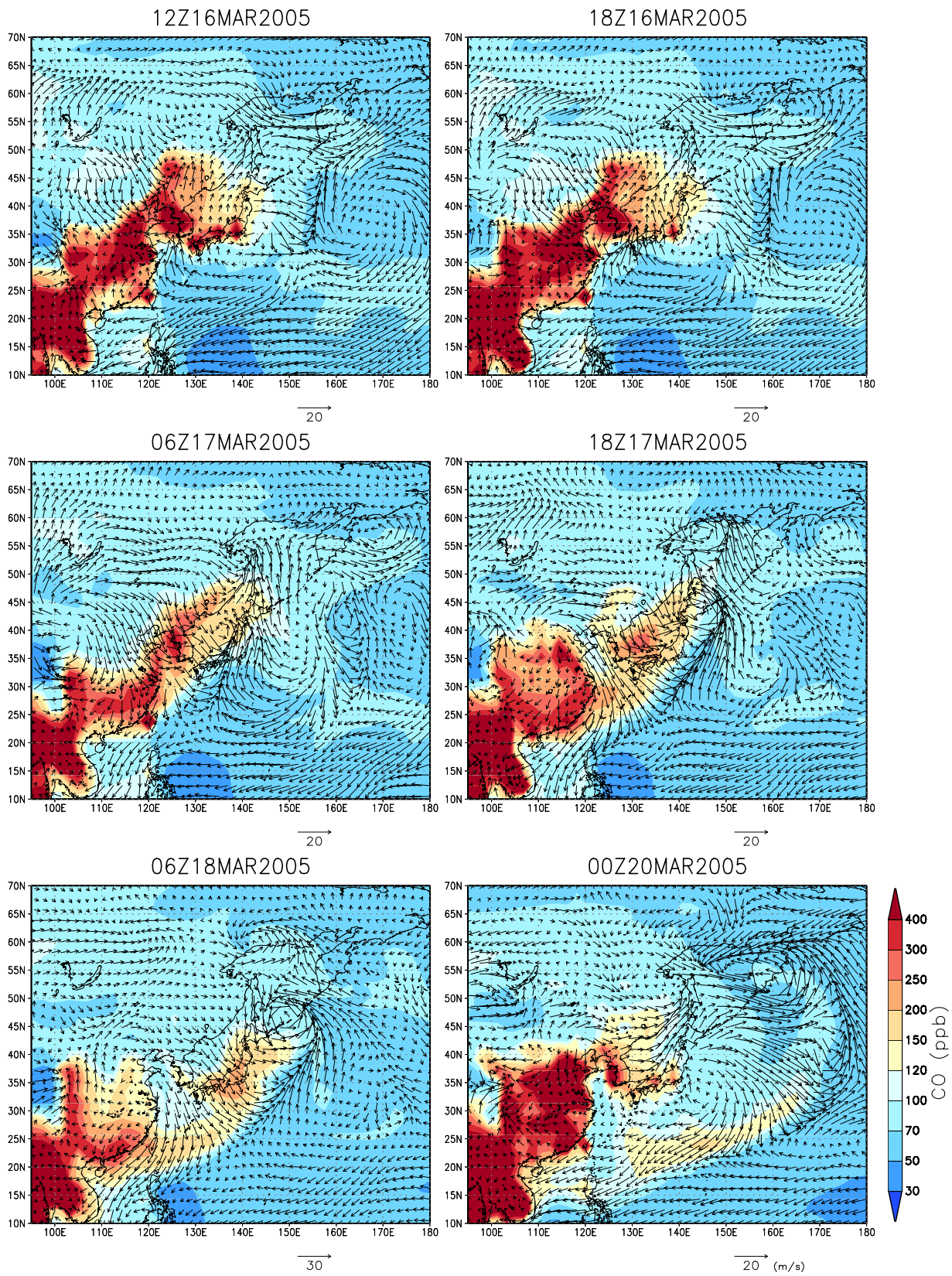
Figure 5. Time series of surface ($\sigma = 0.995$) CO distributions (shaded contours) simulated by the model and wind field (vectors) from 16 to 20 March 2005.
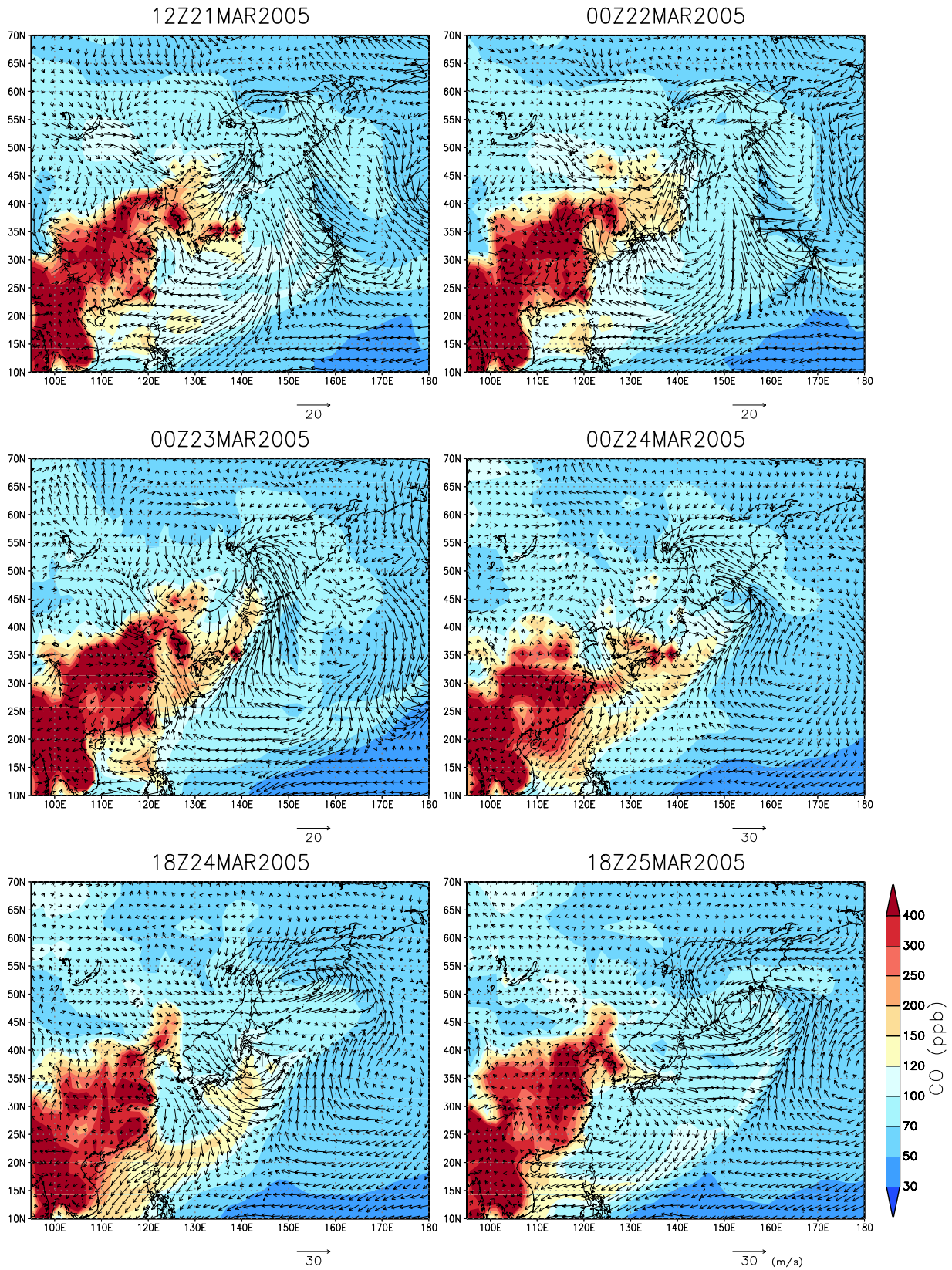
Figure 6. Same as Figure 5 but from 21 to 25 March 2005.
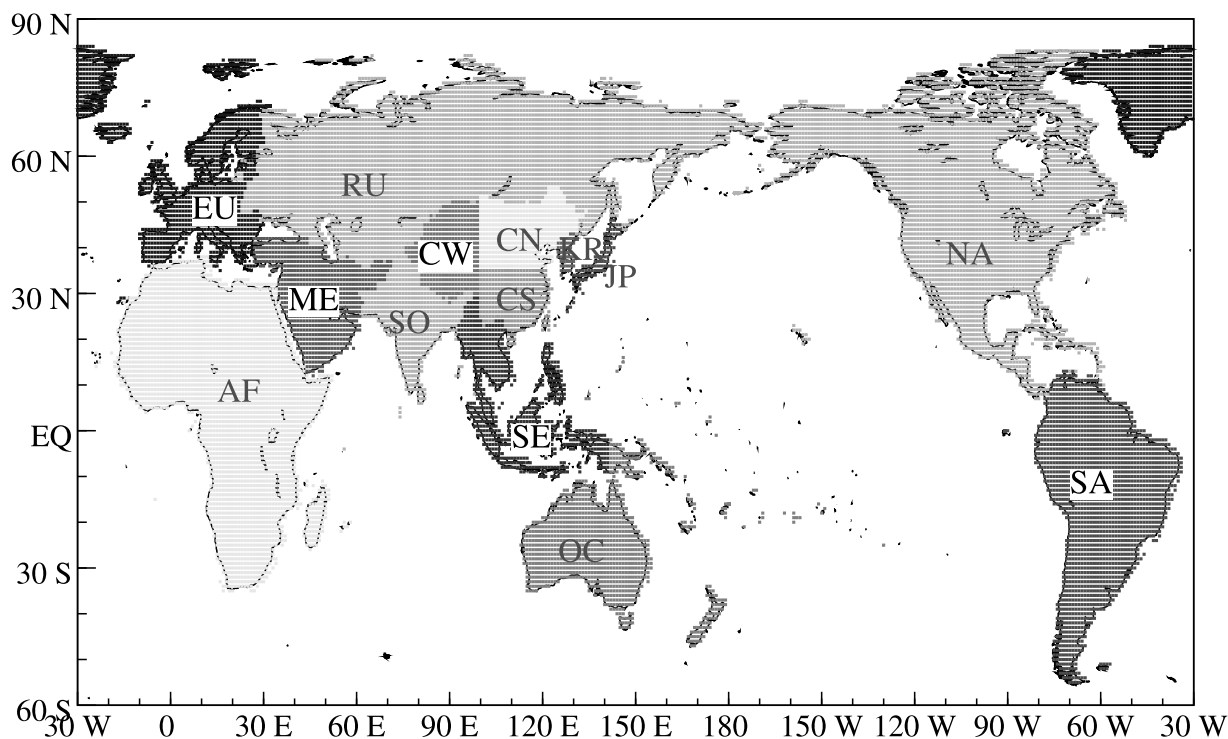
Figure 7. CO tracer regions for the model in this study showing Japan (JP), Korea (KR), northeastern China (CN), southeastern China (CS), western China (CW), Southeast Asia (SE), south Asia (SO), Europe (EU), North America (NA), South America (SA), Russia (RU), Middle East (ME), Africa (AF), and Oceania (OC).

CO peak was observed, corresponding nearly to the time of maximum wind speed behind the cold front. It is suggested that the second CO peak was caused by a relatively large-scale transport of pollutants from the continent. There seems to be a very narrow band of pollution confined to a region immediately behind the cold front, possibly due to a mesoscale circulation convergence. The second peak, as mentioned above, appears to be associated with a more general large-scale transport. In the case of event III, the third CO peak was observed at each of the three stations in the East China Sea, associated again with an increase in wind speed. A small decrease in pressure and an abrupt change in the wind direction associated with event III were observed at Gosan and Fukuejima, but not clearly at Amami-Oshima and Yonagunijima. The third CO peak was likely associated with the development and the movement of the second low (Figure 3c).

[25] Spatiotemporal evolution of the IC events and the associated meteorology observed at the monitoring stations show that a moving frontal system is the major transport mechanism for exporting anthropogenic emissions from the continent to the marine boundary layer over the East China Sea. From shipboard measurements over the East China Sea, *Kaneyasu et al.* [2000], for example, reported similar polluted events with the arrival of cold air and increased wind speeds for sulfur dioxide and black carbon. It was also reported from a model calculation that increased CO in the Asian outflow during the spring season is often driven by the eastward moving cold fronts [*Carmichael et al.*, 1998; *Yienger et al.*, 2000; *Bey et al.*, 2001; *Liu et al.*, 2003; *Uno*

et al., 2003; *Mari et al.*, 2004; *Liang et al.*, 2004]. Our results present observational evidence of the boundary layer transport across the stations over the East China Sea in a wide latitudinal band along the front (24°N–33°N). Although the northerly winds still continued for 1–2 d after each IC event, the mixing ratios of CO returned to the lower levels that existed before the event. These results suggest that the northerly winds brought pollution but the width of the highly polluted air was confined to a region just behind the cold front.

[26] Figure 4e shows the time series of meteorological parameters observed at Minamitorishima. At Minamitorishima, as elsewhere, the increase in CO observed during each of events I, II and III was associated with a change in the wind direction from southerly to northerly, as well as with wind speed increase, that corresponded to a cold frontal passage. In contrast to the stations in the East China Sea, a pressure decrease did not occur when the wind shifted because the northeastward moving low-pressure systems were located in the high latitudes far from the station when cold fronts passed Minamitorishima. The observations of events I, II and III at Minamitorishima demonstrate clearly the effectiveness of a long-range pollution transport by frontal systems. Very few studies have discussed the detailed meteorological situations leading to long-range transport [*Jaffe et al.*, 1998; *Murayama et al.*, 2003], although many previous studies utilizing trajectory analysis have reported the influences of Asian pollution on atmospheric chemistry measurements at remote ocean islands [e.g., *Merrill et al.*, 1989; *Harris et al.*, 1992; *Jaffe et al.*, 1997].
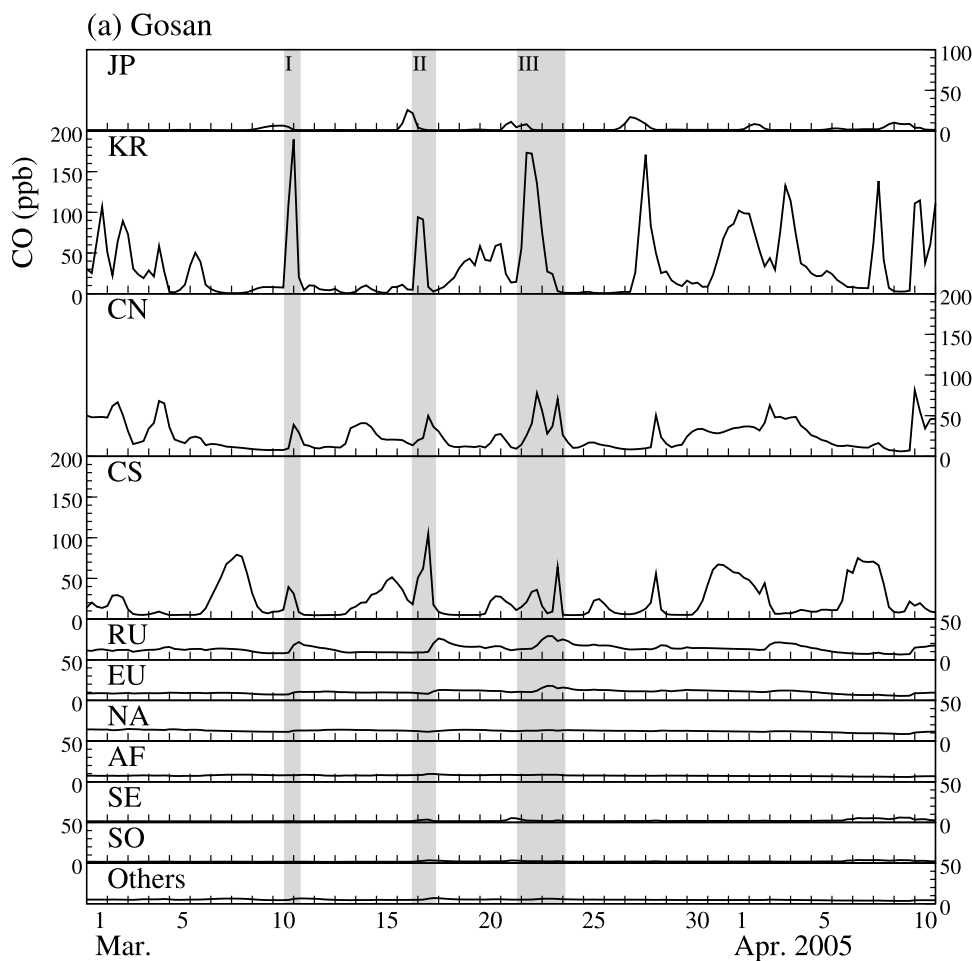
Figure 8a. Simulated CO mixing ratios by the regional tagged CO traces for JP, KR, CN, CS, RU, EU, NA, AF, SE, SO, and other regions (ME, OC, SA, and CW) for Gosan from 1 March to 10 April 2005. Shaded regions indicate the periods of significant enhanced CO events observed at the station.

[27] Wind and pressure time series for the two northern stations of Ryori and Cape Ochi-ishi are shown in Figures 4f and 4g. Although the CO events were associated with similar meteorological conditions as in the southern stations, there are notable differences. For example, the first CO peaks at Ryori and Cape Ochi-ishi appeared before the pressure started to decrease, while the second CO peaks occurred at the time of the pressure minimum. During the first CO peak, southerly winds dominated, although the wind direction was slightly variable caused probably by the topography around the inland stations. This suggests that the CO enhancement of the first peak was caused by the northward advection of large CO emissions from several megacities of Japan, located south of Ryori and Cape Ochi-ishi. This transport process, associated with the general northeastward movement of synoptic weather systems from Japan to the Gulf of Alaska [*Gykum et al.*, 1989], is one of the major processes for exporting pollution from the southern emission regions to the regions in the North Pacific. *Liang et al.* [2004] found the boundary layer transport in the prefrontal jet, a band of high-speed winds ahead of a surface cold front, as a new outflow mechanism for pollution. However, their prefrontal exports occur during seasons other than the spring. Our observational results suggest another important mecha-

nism for northward transport in the boundary layer which allows for a combined effect of storm tracks and large CO emission in the southern regions in east Asia.

3.4. Three-Dimensional Transport Simulation of Polluted Air

[28] The temporal CO variations observed at 7 stations are simulated using a global transport model (dashed lines in Figure 2). The model is generally successful in identifying major IC events observed at all the stations, as well as their timing of occurrences. Since the model is driven by the relatively coarse reanalysis data, it is not able to reproduce the small-scale polluted plumes close to the sources because of the dilution of the emission strength. A relatively constant offset of CO background levels between the model and observation at all of the stations is due mainly to the lack of photochemical oxidation processes in the model calculation. The production of CO from the oxidation processes has been estimated in other studies, although there are some differences in the budget among the models [*Allen et al.*, 1996; *Granier et al.*, 2000; *Pétron et al.*, 2002; *Horowitz et al.*, 2003; *Liang et al.*, 2004; *Wang et al.*, 2004; *Takigawa et al.*, 2005].
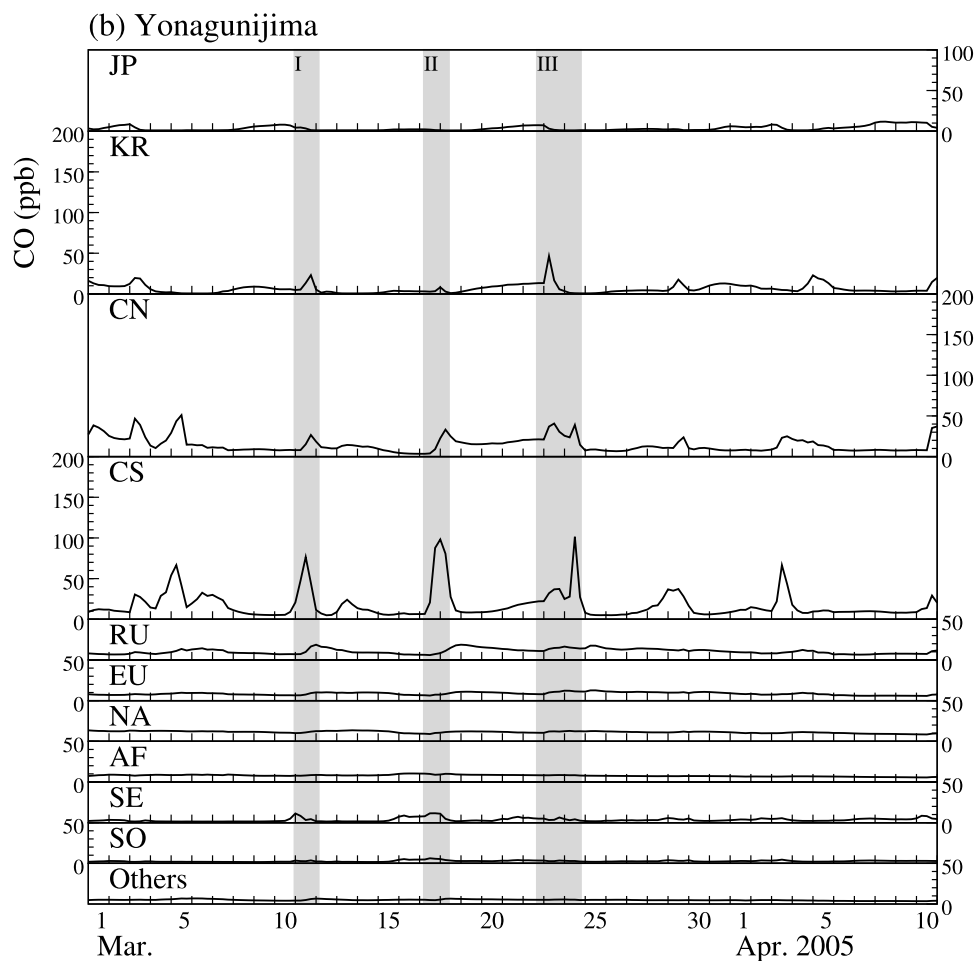
Figure 8b. Same as Figure 8a but for Yonagunijima.

[29] Although the model does relatively well in simulating the timing of the major CO events, it significantly underestimates the magnitude. *Kiley et al.* [2003] also reported that several different models generally tend to underestimate the magnitude of intense CO plumes. The major cause is the uncertainty in the CO emission inventories in the EDGAR database used in this study. *Ma and van Aardenne* [2004] reported that the yearly CO emissions from China for the EDGAR data are smaller by about 30% compared with the database from *Streets et al.* [2003]. In addition, *Palmer et al.* [2003] pointed out that the anthropogenic emissions from China should be increased by 54% relative to the *Streets et al.* [2003] inventory on the basis of an optimal estimation inverse model. Other causes for the underestimation by the model originate partly from the lack of inclusion of photochemical production of CO by rapid oxidations of NMHCs. Although these factors for the underestimation in the model cannot be quantitatively evaluated in the present study, most of the major episodic events observed at 7 stations during EAREX 2005 are identified by our model calculation, as shown in Figure 2. The model results provide useful information for gaining some insight into the mechanism of transport that produced the major episodic CO events observed in the western Pacific during March and early April in 2005.

[30] Figure 5 shows a time change of surface CO and wind vector distributions over the western North Pacific simulated by the 3-D model during 16–20 March associated with event II. It clearly shows the temporal evolution of the CO concentration field over the western North Pacific as it comes off the source regions in Asia.

[31] At 1200 UTC on 16 March, before event II, relatively weak winds are found over the coastal regions, forcing accumulation of CO over the large emission regions in China, Korea, Japan and Southeast Asia. Anticyclonic circulation associated with the high pressure system located south of Japan produces southeasterly winds over the East China Sea, preventing outflow of CO from the source regions on the continent, while allowing CO emissions from central Japan to move gradually northward. By 1800 UTC on 16 March, wind changes direction and now blows from the north over the Yellow Sea between the Korean peninsula and China. As a result of this change, high CO from Korea and China flows out to the Yellow Sea and the Sea of Japan. As the Japanese emissions are transported northward, CO at Cape Ochi-ishi begins to increase at this time. By 0600 UTC on 17 March, a long belt of heavily polluted plumes with enriched CO is formed along the Asian continent and is advected through the Korean peninsula to reach the Gosan and Fukuejima stations. Winds by this time have intensified, blowing southeastward from the
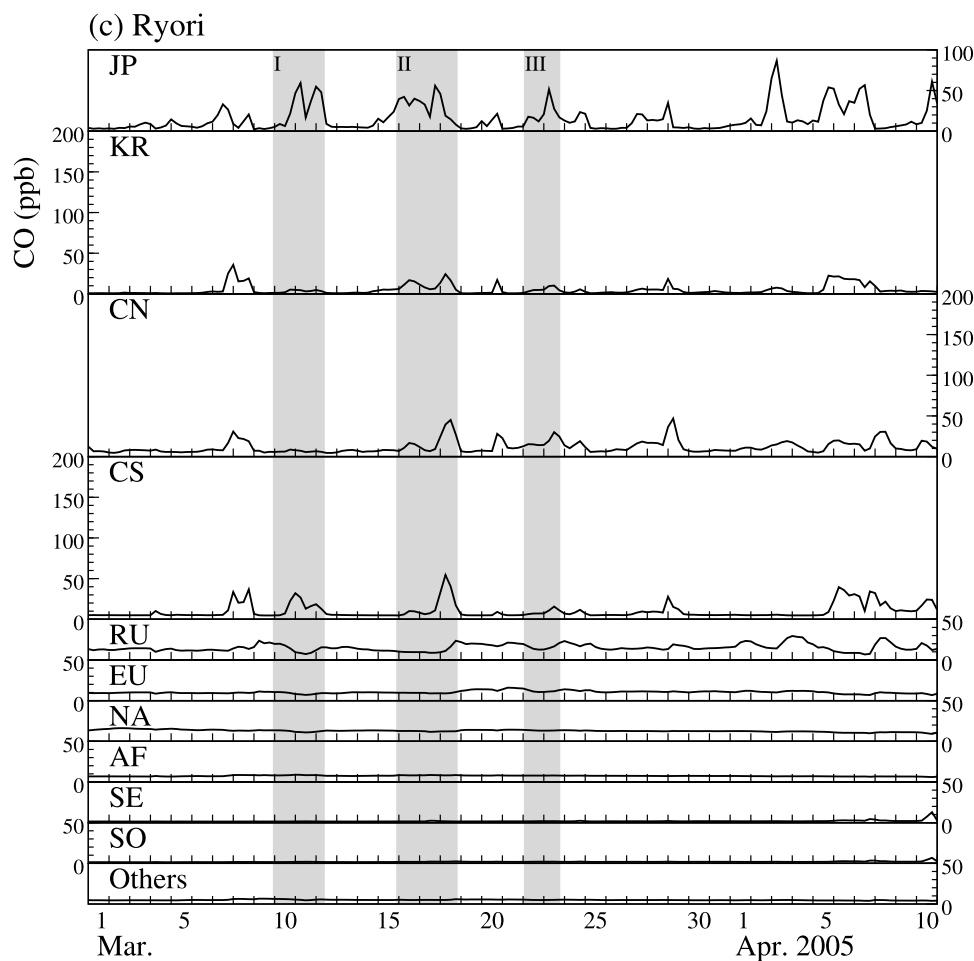
Figure 8c. Same as Figure 8a but for Ryori.

continent to the East China Sea. After 12 h, at 1800 UTC on 17 March, the pollution outflows through the Korea peninsula, spreads out over the Sea of Japan, and then combines with the emissions from central Japan. Another CO-enriched plume from the mid–east coast of China extends toward the middle part of the East China Sea to register a high CO event at Amami-Oshima. At 0600 UTC on 18 March, a strong advection of CO-enriched plumes from the southern part of China can be seen; this leads to an elevation of CO concentration at Yonagunijima. Thus these model results show that the outflow regions for the high CO plumes shifted from the northern to southern parts in the East China Sea for event II.

[32] The regions of high CO concentration continue be advected eastward and southeastward, in response to the circulation associated with the synoptic system. A narrow band of high CO, enhanced by emissions from China, Korea and Japan, is concentrated behind the cold front of the system. After some dilution, this band eventually reaches Minamitorishima, causing slightly enhanced CO observation there (see panels for 18 and 20 March). A synoptic system provides a mechanism for flushing pollution off the Asian continent onto the western North Pacific. Until this flushing effect is provided, pollution accumulates over the source region.

[33] A similar pattern of outflow is simulated for event III (Figure 6). One interesting feature of event III is the influence of the second low system discussed in section 3.2 in producing the third CO peak at Amami-Oshima and Yonagunijima. The panel for 0000 UTC on 24 March clearly shows two CO bands separated by a small clear area south of southern Japan. The model depicts these two bands moving southeastward, with these bands causing the second and the third CO peaks at these two stations. As described earlier, these bands are associated with cold fronts of the first and the second low systems, respectively.

3.5. Source Regions for Enhanced CO

[34] In order to examine the relative impact of different CO source regions on the CO variations observed at the stations along the western North Pacific, model simulations are performed separately for 14 different emission regions, as shown in Figure 7. In particular, east Asia is divided into 5 emission regions of Japan (JP), Korea (KR), northeastern China (CN), southeastern China (CS), and western China (CW), in order to obtain a detailed evaluation of their individual contributions to the episodic CO enhancements. Other Asian emission regions are Southeast Asia (SE) and south Asia (SO). Figures 8a, 8b, 8c, and 8d show CO time variations simulated by the major emission regions for Gosan, Yonagunijima, Ryori and Minamitorishima. All of
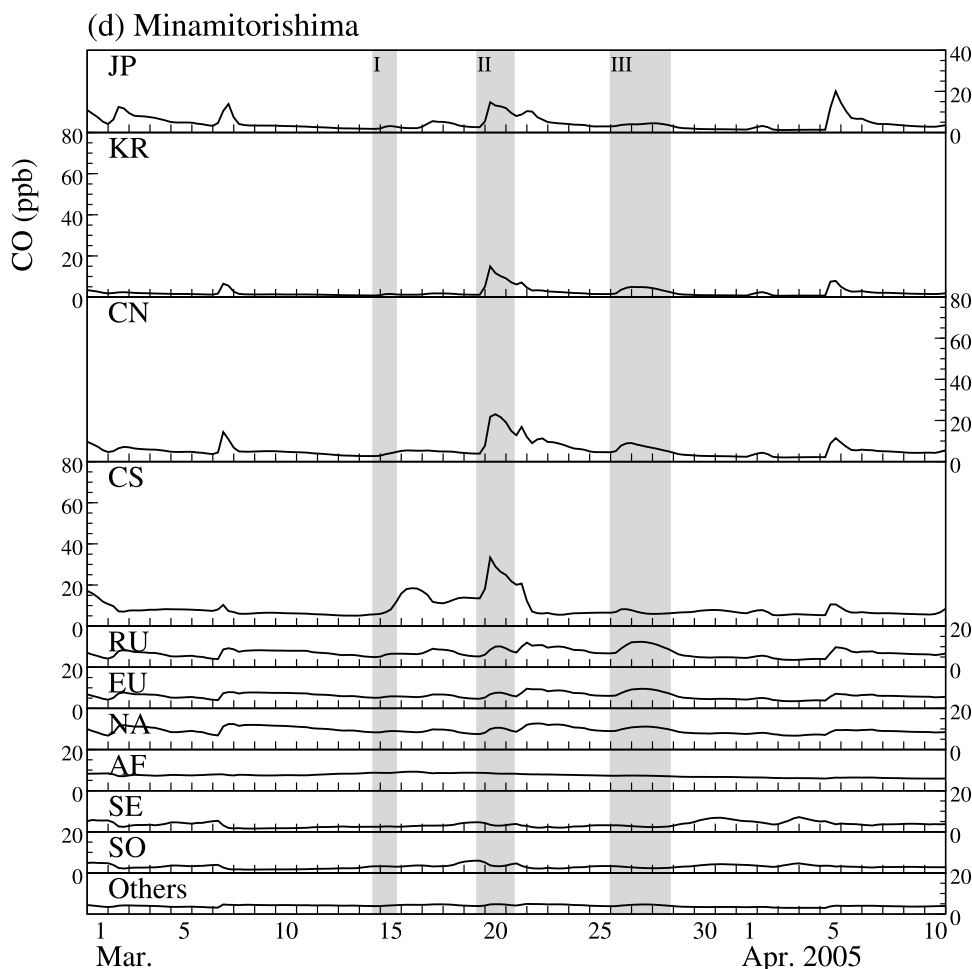
(d) Minamitorishima

Figure 8d. Same as Figure 8a but for Minamitorishima. The *y* axis scale is different from those for Figures 8a–8c.

these stations show a large impact of Asian emissions compared to other anthropogenic CO emission regions such as Europe (EU) and North America (NA). However, the influence of the individual Asian sources depends largely on the geographical location of the observational stations in the western North Pacific.

[35] At Gosan, it is obvious that the CO emissions from KR have contributed significantly to events I, II and III. The CO emissions from CN and CS also produce several CO events at Gosan but they are slightly smaller in magnitude and show delayed arrival time compared to those from KR. There is some visible RU influence as well at Gosan. Emissions from very distant source regions such as EU and NA produce a low but steady background CO concentration. On the other hand, the CS emission region has the largest influence in producing CO pollution events at Yonagunijima, with some influence from KR and CN. As was the case with Gosan, Yonagunijima also sees some influence from RU; this is expected since these two stations are geographically close. However, although not very obvious from the diagram, the contributions from SE and SO are relatively larger at Yonagunijima than at Gosan. Interestingly, the CO enhancement peaks caused by these southern Asia emissions appear just before the CO increases

due to the Chinese emissions, reflecting the influence of relative positions of the emission regions and the transport process. The episodic CO events at Ryori show a major contribution from the JP emission region. The CO peaks due to emissions from Korean and China are relatively reduced and occur after the impact from the Japanese emissions.

[36] Minamitorishima is located far from the continent, and as a result the model simulations of CO events at the station show relatively similar levels of influence from all the Asian source regions at almost the same time. Some contributions from the Eurasian sources are also detectable. As a result of long-range transport of pollutants to a relatively remote location, Minamitorishima sees mixed polluted air masses from various regions of Asia and other regions including Europe and Russia.

3.6. Vertical Structure of Polluted Air Masses

[37] A vertical structure of CO distribution simulated by the model is shown for 0600 UTC on 18 March in Figure 9, along with the corresponding meteorological variables of potential temperature, wet bulb potential temperature and vertical velocity. Wet bulb potential temperature θ_w, which is a useful indicator of air mass in the vicinity of a front [*Browning*, 1990; *Vaughan et al.*, 2003] is calculated from
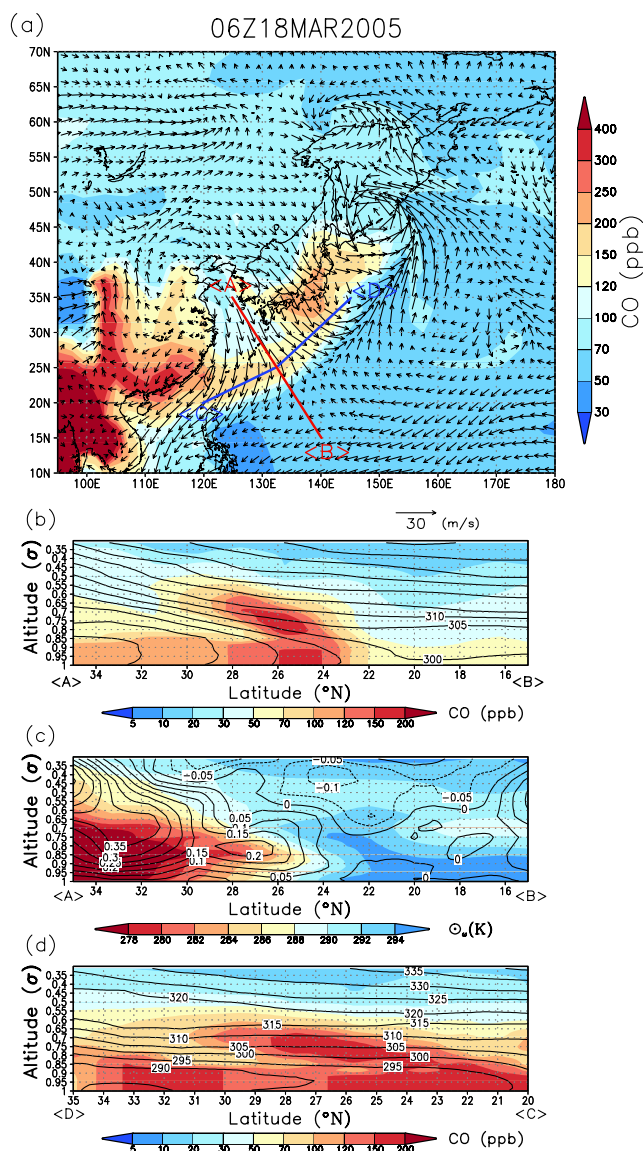
Figure 9. (a) CO distribution simulated by the model and wind field (vectors) for 0600 UTC on 18 March 2005. Thick red and blue lines show the position of cross sections of the lateral and longitudinal to the cold front. (b) Cross section for simulated CO and potential temperature (K) along A-B. (c) Cross section for wet bulb potential temperature θ_w (shaded contour) and omega velocity (Pa/s) along A-B. (d) Cross section for simulated CO and potential temperature along C-D. The x axis is latitude (°N), and the y axis is altitude with σ coordinate (Figures 9b–9d).

one at around 0.8 σ level ($\sim$ about 2 km) above the boundary layer. The surface CO plumes are located near the northerly wind maximum behind the cold front. The omega velocity distribution shown in Figure 9c indicates strong subsidence field that constrains the polluted air masses behind the cold front to the boundary layer. On the other hand, the plume that is located at around 2 km is just above the boundary layer in the frontal zone situated around 24°–28°N. Although there are no observational evidences in the present study, similar outflows of polluted air masses above the boundary layer were reported over the same western North Pacific region during several previous
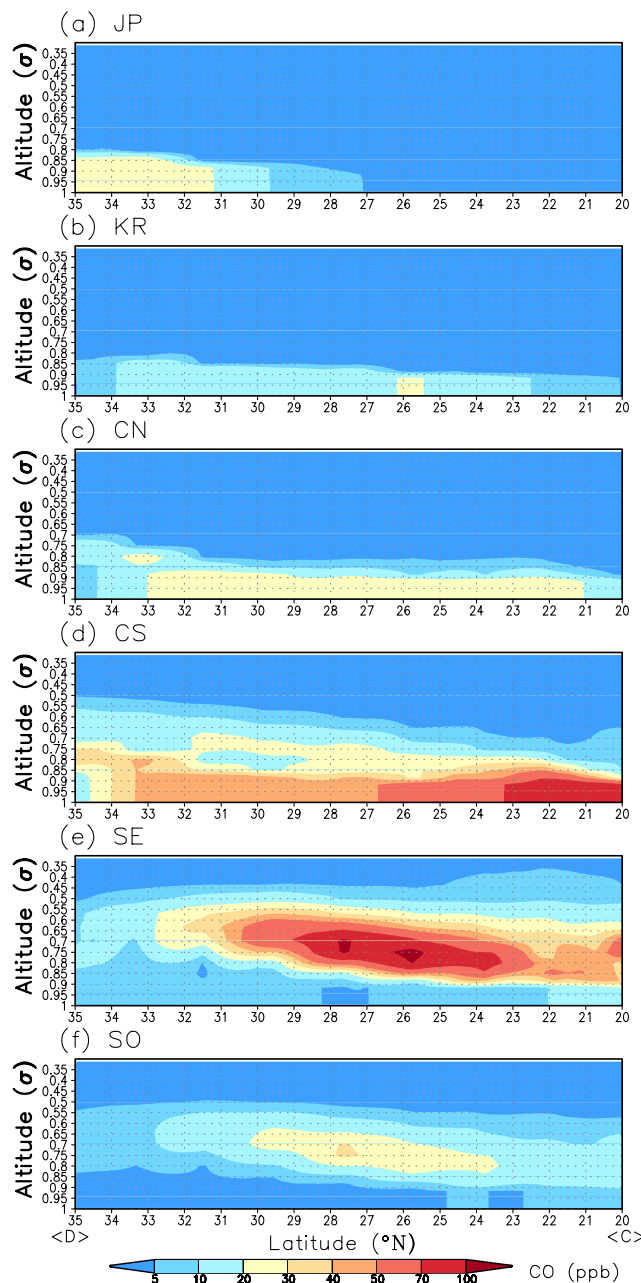
Figure 10. Longitudinal cross section along front C-D in Figure 9a for simulated CO at 0600 UTC on 18 March 2005 for each tagged CO tracer simulation: (a) JP, (b) KR, (c) CN, (d) CS, (e) SE, and (f) SO.

the temperature and humidity data in the reanalysis data. The cold frontal zone appears to be located around 23°N, with θ_w of around 280 K behind the cold front in the colder air mass and of around 294 K in the warmer air mass ahead of the front. The vertical distribution of CO in Figure 9b reflects the slope of the cold front, as it is being advected southeasterly behind the front. The cross-sectional distribution of CO in Figure 9b clearly shows two plumes with concentrated CO above 150 ppb, one located below 0.85 σ level ($\sim$ about 1.5 km) in the boundary layer and another

aircraft campaigns [e.g., *Jacob et al.*, 2003; *Sawa et al.*, 2004; *Oshima et al.*, 2004].

[38] Figure 10 shows the longitudinal cross sections along the transect C-D in Figure 9a, demonstrating the influence of different Asian sources on the altitudinal distribution of CO along the cold front at 0600 UTC on 18 March. Most of the CO emitted from the east Asian sources such as southern China, northern China, Korea, and Japan is confined to the lower altitudes of less than 0.8 σ. The emissions from the southern China have the largest impact in regions south of 23°N, but their influence does stretch across almost the entire transect to 34°N along the cold front. The influence of emissions from northern China shows a similar latitudinal extent, producing a relatively uniform CO concentration along the front (21°N–33°N). The CO distribution from the Korean source is spread relatively uniformly from 23°N to 34°N, while the distribution from the Japanese source is confined to higher latitudes north of 31°N. While the influence on simulated CO concentration field from the east Asian sources is confined mostly to the surface layer behind the cold front, the plumes of CO from south Asia and Southeast Asia are found at higher altitudes near the 0.8 σ level (Figures 10e and 10f). The elevated CO from Southeast Asia is larger than that from south Asia, but the distribution pattern above the boundary layer from 24°N to 28°N is similar in both cases. Since CO plumes above the boundary layer tend to spread along isentropic surfaces from near surface in lower latitudes (Figures 9d, 10d, and 10e), it is possible that the plumes above the boundary layer reflect isentropic transport rather than the above-boundary layer transport. It should be noted, however, that the convective upward transport of polluted air masses is more active in lower-latitude regions than in the midlatitudes of the east Asian regions [e.g., *Miyazaki et al.*, 2003]. It is therefore easier for CO from the surface in regions such as SE and SO to be convectively carried above the boundary layer and then horizontally transported northward. Quantitative details of the actual mechanism are now being investigated.

4. Summary

[39] We have examined the pollution outflow from the Asian continent during the EAREX 2005 campaign in March 2005 using high-resolution CO data obtained at 7 surface stations in the western North Pacific. For this period, three major CO events were identified at 4 southern stations (Gosan, Fukuejima, Amami-Oshima, and Yonaguni-jima) in the East China Sea for a detailed analysis of a widespread outflow of continental air pollution. The movement of CO from Gosan to the East China Sea took about half a day to 1 d. The transport associated with each major pollution event involved circulation around a migratory synoptic system, and in particular advection behind the cold front. When a frontal system passed over a station located in the East China Sea, corresponding changes in wind and pressure were observed, along with occurrences of high CO concentration peaks. These observations suggested a postfrontal transport of CO from emission regions to the southern stations in the East China Sea. On the other hand, northward transport by the circulation around a low-pressure system provided a major transport mechanism for each of the

major events observed at the northern Japanese stations of Ryori and Ochi-ishi. Unlike the southern stations, these stations saw significant influence from the CO emissions in Japan. Because of the long distance of the location of Minamitorishima from the Asian continent, a CO event associated with frontal transport was observed at the station 3–4 d after it was detected by the stations in the East China Sea.

[40] A three-dimensional atmospheric transport model was used to simulate the observed major CO events, and to obtain some insight into the long-range transport by a frontal system. The model was used also to obtain estimates of relative contributions of various CO sources made to the CO events observed at the monitoring stations. The model simulated well the confinement of polluted air behind a cold front, and its advection from the Asian continent as it was transported by the southeasterly movement of the cold front. The frontal system provided a flushing mechanism to push out polluted air from the source regions.

[41] Relative contributions of 14 different emission regions to the CO concentration field along the cold front were then examined. Emissions from southern China had the largest influence from 20°N to 34°N, although a region of maximum CO was found in lower latitudes south of 23°N. Northern China and Korea also showed wide influences, while Japan had impacts on regions located at relatively higher latitudes north of 25°N. Influences from these four emission regions in east Asia were found only in the boundary layer, but CO emitted from Southeast Asia and south Asia was found in higher altitudes above the boundary layer.

[42] In this study, a well-coordinated observed data set combined with model simulations provided additional evidence that migratory cyclones play an important role in producing a widespread air pollution over the western North Pacific by transporting polluted air masses from various CO source regions in Asia. However, since the study period related to the EAREX 2005 campaign was only about a month long in the spring, further work is needed to better understand the Asian outflow over the western North Pacific on a longer time period. Also, the temporal evolution of the mesoscale structure of the CO distribution behind a cold front observed in this study requires a detailed quantitative analysis.

References

Akimoto, H., et al. (1996), Long-range transport of ozone in the east Asia Pacific rim region, *J. Geophys. Res.*, *101*(D1), 1999–2010.
Allen, D. J., P. Kasibhatla, A. M. Thompson, R. B. Rood, B. G. Doddridge, K. E. Pickering, R. D. Hudson, and S.-J. Lin (1996), Transport-induced

interannual variability of carbon monoxide determined using a chemistry and transport model, *J. Geophys. Res.*, *101*(D22), 28,665–28,669.

Bey, I., D. J. Jacob, J. A. Logan, and R. M. Yantosca (2001), Asian chemical outflow to the Pacific in spring: Origins, pathways, and budgets, *J. Geophys. Res.*, *106*(D19), 23,097–23,113.

Browell, E. V., et al. (2003), Large-scale ozone and aerosol distributions, air mass characteristics, and ozone fluxes over the western Pacific Ocean in late winter/early spring, *J. Geophys. Res.*, *108*(D20), 8805, doi:10.1029/2002JD003290.

Browning, K. A. (1990), Organization of clouds and precipitation in *Extratropical Cyclones: The Erik Palmen Memorial Volume*, edited by C. Newton and E. O. Holopainen, pp. 129–153, Am. Meteorol. Soc., Boston, Mass.

Carmichael, G. R., I. Uno, M. J. Phadnis, Y. Zhang, and Y. Sunwoo (1998), Tropospheric ozone production and transport in the springtime in east Asia, *J. Geophys. Res.*, *103*(D9), 10,649–10,671.

Chung, K. K., J. C. L. Chan, C. N. Ng, K. S. Lam, and T. Wang (1999), Synoptic conditions associated with high carbon monoxide episodes at a coastal station in Hong Kong, *Atmos. Environ.*, *33*, 3087–3095.

Cooper, O. R., et al. (2004), A case study of transpacific warm conveyor belt transport: Influence of merging airstreams on trace gas import to North America, *J. Geophys. Res.*, *109*, D23S08, doi:10.1029/2003JD003624.

Crawford, J. H., et al. (1997), Implications of large scale shifts in tropospheric NO$_x$ levels in the remote tropical Pacific, *J. Geophys. Res.*, *102*(D23), 28,447–28,468.

Folkins, I., R. Chatfield, D. Baumgardner, and M. Profitt (1997), Biomass burning and deep convection in southeast Asia: Results from ASHOE/MAESA, *J. Geophys. Res.*, *102*(D11), 13,291–13,299.

Granier, C., G. Pétron, J.-F. Müller, and G. Brasseur (2000), The impact of natural and anthropogenic hydrocarbons on the tropospheric budget of carbon monoxide, *Atmos. Environ.*, *34*, 5255–5270.

Gykum, J. R., J. R. Anderson, R. H. Grumm, and E. L. Gruner (1989), North Pacific cold-season surface cyclone activity: 1975–1983, *Mon. Weather Rev.*, *117*, 1141–1155.

Harris, J. M., P. P. Tans, E. J. Dlugokencky, K. A. Masarie, P. M. Lang, S. Whitestone, and L. P. Steele (1992), Variations in atmospheric methane at Mauna Loa observatory related to long-range transport, *J. Geophys. Res.*, *97*(D5), 6003–6010.

Haurwitz, B., and D. Cowley (1973), The diurnal and semidiurnal barometric oscillations, global distribution and annual variation, *Pure Appl. Geophys.*, *102*, 193–222.

Hoell, J. M., D. D. Davis, S. C. Liu, R. Newell, M. Shipham, H. Akimoto, R. J. McNeal, R. J. Bendura, and J. W. Drewry (1996), Pacific Exploratory Mission-West A (PEM-WEST A): September-October 1991, *J. Geophys. Res.*, *101*(D1), 1641–1653.

Hoell, J. M., D. D. Davis, S. C. Liu, R. Newell, H. Akimoto, R. J. McNeal, and R. J. Bendura (1997), The Pacific Exploratory Mission-West Phase B: February-March 1994, *J. Geophys. Res.*, *102*(D23), 28,223–28,239.

Horowitz, L. W., et al. (2003), A global simulation of tropospheric ozone and related tracers: Description and evaluation of MOZART, version 2, *J. Geophys. Res.*, *108*(D24), 4784, doi:10.1029/2002JD002853.

Hoskins, B. J., and K. I. Hodges (2002), New perspective on the Northern Hemisphere winter storm tracks, *J. Atmos. Sci.*, *59*, 1041–1061.

Huebert, B. J., T. Bates, P. B. Russell, G. Shi, Y. J. Kim, K. Kawamura, G. Carmichael, and T. Nakajima (2003), An overview of ACE-Asia: Strategies for quantifying the relationships between Asian aerosols and their climatic impacts, *J. Geophys. Res.*, *108*(D23), 8633, doi:10.1029/2003JD003550.

Jacob, D. J., J. H. Crawford, M. M. Kleb, V. E. Connors, R. J. Bendura, J. L. Raper, G. W. Sachse, and J. C. Gille (2003), The Transport and Chemical Evolution over the Pacific (TRACE-P) aircraft mission: Design, execution, and first results, *J. Geophys. Res.*, *108*(D20), 9000, doi:10.1029/2002JD003276.

Jaffe, D. A., R. E. Honrath, L. Zhang, H. Akimoto, A. Shimizu, H. Mukai, K. Murano, S. Hatakeyama, and J. Merrill (1996), Measurements of NO, NO$_y$, CO and O$_3$ and estimation of the ozone production rate at Oki Island, Japan, during PEM-West, *J. Geophys. Res.*, *101*(D1), 2037–2048.

Jaffe, D., A. Mahura, J. Kelley, J. Atkins, P. C. Novelli, and J. Merrill (1997), Impact of Asia emissions on the remote North Pacific atmosphere: Interpretation of CO data from Shemya, Guam, Midway and Mauna Loa, *J. Geophys. Res.*, *102*(D23), 28,627–28,635.

Jaffe, D., L. Yurganov, E. Pullman, J. Reuter, A. Mahura, and P. Novelli (1998), Measurements of CO and O$_3$ at Shemya, Alaska, *J. Geophys. Res.*, *103*(D1), 1493–1502.

Japan Meteorological Agency (JMA) (1994), Summary report on the background air pollution monitoring (in Japanese), *Weather Serv. Bull.*, *61*, 145–179.

Japan Meteorological Agency (JMA) (2005a), Monthly report of the Japan Meteorological Agency, February 2005, March 2005, April 2005 [CD-ROM], Jpn. Meteorol. Agency, Tokyo.

Japan Meteorological Agency (JMA) (2005b), Japan Meteorological Agency Weather Charts, March 2005, [CD-ROM], Jpn. Meteorol. Agency, Tokyo.

Kajii, Y., H. Akimoto, Y. Komazaki, S. Tanaka, H. Mukai, K. Murano, and J. T. Merrill (1997), Long-range transport of ozone, carbon monoxide, and acidic trace gases at Oki Island, Japan, during PEM-WEST B/PEACAMPOT B campaign, *J. Geophys. Res.*, *102*(D23), 28,637–28,649.

Kaneyasu, N., K. Takeuchi, M. Hayashi, S. Fujita, I. Uno, and H. Sasaki (2000), Outflow patterns of pollutants from east Asia to the North Pacific in the winter monsoon, *J. Geophys. Res.*, *105*(D13), 17,361–17,377.

Kato, N., and H. Akimoto (1992), Anthropogenic emissions of SO$_2$ and NO$_x$ in Asia: Emission inventories, *Atmos. Environ.*, *26*, 2997–3017.

Kiley, C. M., et al. (2003), An intercomparison and evaluation of aircraft-derived and simulated CO from seven chemical transport models during the TRACE-P experiment, *J. Geophys. Res.*, *108*(D21), 8819, doi:10.1029/2002JD003089.

Kondo, Y., M. Ko, M. Koike, S. Kawakami, and T. Ogawa (2002), Preface to special section on Biomass Burning and Lightning Experiment (BIBLE), *J. Geophys. Res.*, *107*, 8397, doi:10.1029/2002JD002401, [printed *108*(D3), 2003].

Kondo, Y., et al. (2004), Photochemistry of ozone over the western Pacific from winter to spring, *J. Geophys. Res.*, *109*, D23S02, doi:10.1029/2004JD004871.

Liang, Q., L. Laeglé, D. A. Jaffe, P. Weiss-Penzias, and A. Heckman (2004), Long-range transport of Asian pollution to the northeast Pacific: Seasonal variations and transport pathways of carbon monoxide, *J. Geophys. Res.*, *109*, D23S07, doi:10.1029/2003JD004402.

Liu, C.-M., M. Buhr, and J. T. Merrill (1997), Ground-based observation of ozone, carbon monoxide, and sulfur dioxide at Kenting, Taiwan, during the PEM-West B campaign, *J. Geophys. Res.*, *102*(D23), 28,613–28,625.

Liu, H., D. J. Jacob, I. Bey, R. M. Yantosca, B. N. Duncan, and G. W. Sachse (2003), Transport pathways for Asian pollution outflow over the Pacific: International and seasonal variations, *J. Geophys. Res.*, *108*(D20), 8786, doi:10.1029/2002JD003102.

Ma, J., and J. A. van Aardenne (2004), Impact of different emission inventories on simulated tropospheric ozone over China: A region chemical transport model evaluation, *Atmos. Chem. Phys. Discuss.*, *4*, 507–532.

Mari, C., M. J. Evans, P. I. Palmer, D. J. Jacob, and G. W. Sachse (2004), Export of Asian pollution during two cold front episodes of the TRACE-P experiment, *J. Geophys. Res.*, *109*, D15S17, doi:10.1029/2003JD004307.

Matsueda, H., H. Y. Inoue, Y. Sawa, and Y. Tsutsumi (1998), Carbon monoxide in the upper troposphere over the western Pacific between 1993 and 1996, *J. Geophys. Res.*, *103*(D15), 19,093–19,110.

Merrill, J. T., M. Uematsu, and R. Bleck (1989), Meteorological analysis of long range transport of mineral aerosols over the North Pacific, *J. Geophys. Res.*, *94*(D6), 8584–8598.

Miyazaki, Y., et al. (2003), Synoptic-scale transport of reactive nitrogen over the western Pacific in spring, *J. Geophys. Res.*, *108*(D20), 8788, doi:10.1029/2002JD003248.

Murayama, S., K. Harada, K. Gotoh, T. Kitao, T. Watai, and S. Yamamoto (2003), On large variations in atmospheric CO$_2$ concentrations observed over the central and western Pacific Ocean, *J. Geophys. Res.*, *108*(D8), 4243, doi:10.1029/2002JD002729.

Nakajima, T., and S.-C. Yoon (Eds.) (2005), *Implementation Plan for ABC Gosan Campaign: East Asia Regional Experiment 2005*, 73 pp., Sch. of Earth and Environ. Sci., Seoul Natl. Univ., Seoul.

Nam, J. C., and S. Y. Bang (2005), Introduction of meteorological information for ABC-Gosan campaign, paper presented at 1st ABC-EAREX 2005 Data Analysis Workshop, Res. Inst. for Hum. and Nature, Kyoto, Japan, 29 June to 1 July .

Novelli, P. C., L. P. Steele, and P. P. Tans (1992), Mixing ratios of carbon monoxide in the troposphere, *J. Geophys. Res.*, *97*(D18), 20,731–20,750.

Novelli, P. C., et al. (1998), An internally consistent set of globally distributed atmospheric carbon monoxide mixing ratios developed using results from an intercomparison of measurements, *J. Geophys. Res.*, *103*(D15), 19,285–19,293.

Novelli, P. C., K. A. Masarie, P. M. Lang, B. D. Hall, R. C. Myers, and J. W. Elkins (2003), Reanalysis of tropospheric CO trends: Effects of the 1997–1998 wildfires, *J. Geophys. Res.*, *108*(D15), 4464, doi:10.1029/2002JD003031.

Olivier, J. G. J., and J. J. M. Berdowski (2001), Global emissions sources and sinks, in *The Climate System*, edited by J. Berdowski, et al., pp. 33–78, Taylor and Francis, Philadelphia, Pa.

Olivier, J. G. J., J. P. J. Bloos, J. J. M. Berdowski, A. J. H. Visschedijk, and A. F. Bouwman (1999), A 1990 global emission inventory of anthropo-

genic sources of carbon monoxide on $1° \times 1°$ developed in the framework of EDGAR/GEIA, *Chemosphere Global Change Sci.*, 1, 1–17.

Olivier, J. G. J., Van J. A. Aardenne, F. Dentener, L. Ganzeveld, and J. A. H. W. Peters (2005), Recent trends in global greenhouse gas emissions: Regional trends and spatial distribution of key sources, in *Non-CO₂ Greenhouse Gas Emissions* (NCGG-4), edited by A. van Amstel, pp. 325–330, Millpress, Rotterdam, Netherlands.

Oshima, N., et al. (2004), Asian chemical outflow to the Pacific in late spring observed during the PEACE-B aircraft mission, *J. Geophys. Res.*, 109, D23S05, doi:10.1029/2004JD004976.

Palmer, P. I., D. J. Jacob, D. B. A. Jones, C. L. Heald, R. M. Yantosca, J. A. Logan, G. W. Sachse, and D. G. Streets (2003), Inverting for emissions of carbon monoxide from Asia using aircraft observations over the western Pacific, *J. Geophys. Res.*, 108(D21), 8828, doi:10.1029/2003JD003397.

Pétron, G., C. Granier, B. Khattatov, J.-F. Lamarque, V. Yudin, J.-F. Müller, and J. Gille (2002), Inverse modeling of carbon monoxide surface emissions using Climate Monitoring and Diagnostics Laboratory network observations, *J. Geophys. Res.*, 107(D24), 4761, doi:10.1029/2001JD001305.

Pochanart, P., J. Hirokawa, Y. Kajii, H. Akimoto, and M. Nakao (1999), Influence of regional-scale anthropogenic activity in northeast Asia on seasonal variations of surface ozone and carbon monoxide observed at Oki, Japan, *J. Geophys. Res.*, 104(D3), 3621–3631.

Ramanathan, V., and P. J. Crutzen (2003), New directions: Atmospheric brown "clouds", *Atmos. Environ.*, 37, 4033–4035.

Sawa, Y. (2005), A study of variations and transport of carbon monoxide in the free troposphere over the western Pacific, Ph.D. thesis, 184 pp., Tohoku Univ., Sendai, Japan.

Sawa, Y., H. Matsueda, Y. Makino, H. Y. Inoue, S. Murayama, M. Hirota, Y. Tsutsumi, Y. Zaisen, M. Ikegami, and K. Okada (2004), Aircraft observation of CO₂, CO, O₃ and H₂ over the North Pacific during the PACE-7 campaign, *Tellus, Ser. B*, 56, 2–20.

Spivakovsky, C. M., et al. (2000), Three-dimensional climatological distribution of tropospheric OH: Update and evaluation, *J. Geophys. Res.*, 105(D7), 8931–8980.

Stohl, A. (2001), A 1-year Lagrangian climatology of airstreams in the Northern Hemisphere troposphere and lowermost stratosphere, *J. Geophys. Res.*, 106(D7), 7263–7279.

Streets, D. G., K. Jiang, X. Hu, J. E. Sinton, X.-Q. Zhang, D. Xu, M. Z. Jacobson, and J. E. Hansen (2001a), Recent reductions in China's greenhouse gas emissions, *Science*, 294, 1835–1837.

Streets, D. G., N. Y. Tsai, H. Akimoto, and K. Oka (2001b), Trends in emissions of acidifying species in Asia, 1985–1997, *Water Air Soil Pollut.*, 130, 187–192.

Streets, D. G., et al. (2003), An inventory of gaseous and primary aerosol emissions in Asia in the year 2000, *J. Geophys. Res.*, 108(D21), 8809, doi:10.1029/2002JD003093.

Taguchi, S. (1996), A three-dimensional model of atmospheric CO₂ transport based on analyzed winds: Model description and simulation results for TRANSCOM (1996), *J. Geophys. Res.*, 101(D10), 15,099–15,109.

Taguchi, S., H. Matsueda, H. Y. Inoue, and Y. Sawa (2002a), Long-range transport of carbon monoxide from tropical ground to upper troposphere: A case study for South east Asia in October 1997, *Tellus, Ser. B*, 54, 22–40.

Taguchi, S., T. Iida, and J. Moriizumi (2002b), Evaluation of the atmospheric transport NIRE-CTM-96 using measured radon-222 concentrations, *Tellus, Ser. B*, 54, 250–268.

Takigawa, M., K. Sudo, H. Akimoto, K. Kita, N. Takegawa, Y. Kondo, and M. Takahashi (2005), Estimation of the contribution of international transport during the PEACE campaign by using a global model, *J. Geophys. Res.*, 110, D21313, doi:10.1029/2005JD006226.

Talbot, R. W., et al. (1997), Chemical characteristics of continental outflow from Asia to the troposphere over the western Pacific Ocean during February–March 1994: Results from PEM-West B, *J. Geophys. Res.*, 102(D23), 28,255–28,274.

Tanimoto, H., Y. Kajii, J. Hirokawa, H. Akimoto, and N. P. Minko (2000), The atmospheric impact of boreal forest fires in far eastern Siberia on the seasonal variation of carbon monoxide: Observations at Rishiri, a northern remote island in Japan, *Geophys. Res. Lett.*, 27, 4073–4076.

Tanimoto, H., H. Furutani, S. Kato, J. Matsumoto, Y. Makide, and H. Akimoto (2002), Seasonal cycles of ozone and oxidized nitrogen species in northeast Asia: 1. Impact of regional climatology and photochemistry observed during RISOTTO 1999–2000, *J. Geophys. Res.*, 107(D24), 4747, doi:10.1029/2001JD001496.

Tanimoto, H., Y. Sawa, H. Matsueda, I. Uno, T. Ohara, K. Yamaji, J. Kurokawa, and S. Yonemura (2005), Significant latitudinal gradient in the surface ozone spring maximum over east Asia, *Geophys. Res. Lett.*, 31, L16106, doi:10.1029/2004GL020093.

Tanimoto, H., et al. (2007), Direct assessment of international consistency of standards for ground-level ozone: Strategy and implementation toward metrological traceability network in Asia, *J. Environ. Monit*, doi:10.1039/b701230f.

Tohjima, Y., T. Machida, M. Utiyama, M. Katsumoto, Y. Fujinuma, and S. Maksyutov (2002), Analysis and presentation of in situ atmospheric methane measurements from Cape Ochi-ishi and Hateruma Island, *J. Geophys. Res.*, 107(D12), 4148, doi:10.1029/2001JD001003.

Troen, I., and L. Mahrt (1986), A simple model of the atmosphere boundary layer, sensitively to surface evaporation, *Boundary Layer Meteorol.*, 37, 129–148.

Uno, I., et al. (2003), Regional chemical weather forecasting system CFORS: Model descriptions and analysis of surface observations at Japanese island stations during the ACE-Asia experiment, *J. Geophys. Res.*, 108(D23), 8668, doi:10.1029/2002JD002845.

Vaughan, G., W. E. Garland, K. J. Dewey, and C. Gerbig (2003), Aircraft measurements of a warm conveyor belt–A case study, *J. Atmos. Chem.*, 46, 117–129.

Wang, Y. X., M. B. McElroy, T. Wang, and P. I. Palmer (2004), Asian emissions of CO and NOₓ: Constraints from aircraft and Chinese station data, *J. Geophys. Res.*, 109, D24304, doi:10.1029/2004JD005250.

Watanabe, F., O. Uchino, Y. Joo, M. Aono, K. Higashijima, Y. Hirano, K. Tsuboi, and K. Suda (2000), Interannual variation of growth rate of atmospheric carbon dioxide concentration observed at the JMA's three monitoring stations: Large increase in concentration of atmospheric carbon dioxide in 1998, *J. Meteorol. Soc. Jpn.*, 78, 673–682.

Yamada, H. (1999), Observations of greenhouse gases at Yonagunijima in 1997 (in Japanese), *Okinawa Tech. Note 53*, pp. 21–26, Okinawa Meteorol. Obs., Naha, Japan.

Yienger, J. J., M. Galanter, T. A. Holloway, M. J. Phadnis, S. K. Guttikunda, G. R. Carmichael, W. J. Moxim, and H. Levy II (2000), The episodic nature of air pollution transport from Asia to North America, *J. Geophys. Res.*, 105(D22), 26,931–26,945.

─────────────

T. Hayasaka and S. Katagiri, Research Institute for Humanity and Nature, 335 Takashima-cho, Kyoto 602-0878, Japan.

N. Kikuchi, Earth Observation Research Center, Japan Aerospace Exploration Agency, 2-1-1 Sengen, Tsukuba, Ibaraki 305-8505, Japan.

H. Matsueda, Y. Sawa, and A. Wada, Geochemical Research Department, Meteorological Research Institute, 1-1 Nagamine, Tsukuba, Ibaraki 305-0035, Japan. (ysawa@mri-jma.go.jp)

H. Mukai, Center for Global Environmental Research, Institute for Environmental Management Technology, National Institute for Environmental Studies, 16-2 Onogawa, Tsukuba, Ibaraki 305-8506, Japan.

S. Taguchi, Research Institute for Environmental Management Technology, National Institute of Advanced Industrial Science and Technology, 16-1 Onogawa, Tsukuba, Ibaraki 305-8569, Japan.

H. Tanimoto and Y. Tohjima, Atmospheric Environmental Division, National Institute for Environmental Studies, 16-2 Onogawa, Tsukuba, Ibaraki 305-8506, Japan.

K. Tsuboi, Atmospheric Environmental Division, Japan Meteorological Agency, 1-3-4 Otemachi, Chiyoda-ku, Tokyo 100-8122, Japan.

H. Tsuruta, Center for Climate System Research, University of Tokyo, 3-1-3 Kannondai, Meguro-ku, Kashiwa, Chiba 153-8904, Japan.

S. Yonemura, National Institute for Agro-Environmental Sciences, 3-1-3 Kannondai, Tsukuba, Ibaraki 305-8604, Japan.